

# Skin-Mountable Functional Electronic Materials for Bio-Integrated Devices

Jin Young Oh,\* Yeongjun Lee, and Tae-Woo Lee\*

Skin-mountable electronic materials are being intensively evaluated for use in bio-integrated devices that can mutually interact with the human body. Over the past decade, functional electronic materials inspired by the skin are developed with new functionalities to address the limitations of traditional electronic materials for bio-integrated devices. Herein, the recent progress in skin-mountable functional electronic materials for skin-like electronics is introduced with a focus on five perspectives that entail essential functionalities: stretchability, self-healing ability, biocompatibility, breathability, and biodegradability. All functionalities are advanced with each strategy through rational material designs. The skin-mountable functional materials enable the fabrication of bio-integrated electronic devices, which can lead to new paradigms of electronics combining with the human body.

form factors.<sup>[1–5]</sup> Beyond mobile phones, bio-integrated devices that can be combined with the human body in the aspects of software and hardware have received considerable attention as a new device form factor.<sup>[6–10]</sup> Bio-integrated devices on the skin require a new skin-like form factor to stably and mutually interact with our body, which can provide unprecedented abilities to humans.<sup>[9–12]</sup> This could possibly lead to a big paradigm shift in human evolution, which means that humans could choose a man-made strategy for evolution rather than a natural evolution strategy.<sup>[13–15]</sup>

Bio-integrated devices can operate on various surfaces of the human body, akin to a supplementary layer of skin (electronic skin, e-skin). Their successful integration necessitates the development

of suitable skin-mountable functional materials that can seamlessly merge with the human body as a secondary skin.<sup>[2,3]</sup> The required functionalities of electronic materials for bio-integrated skin devices have been categorized into five traits<sup>[16,17]</sup>: 1) stretchability<sup>[18,19]</sup> 2) self-healing ability,<sup>[20,21]</sup> 3) biocompatibility<sup>[22]</sup>, 4) breathability<sup>[23–27]</sup>, and 5) biodegradability<sup>[28]</sup> (Figure 1), which are briefly described as follows.

Stretchability is required for the mechanical compliance of bio-integrated devices with the dynamic surface of the body. Conventional electronic materials such as silicone, metals, and oxides are rigid or brittle. Therefore, they are not appropriate for use in skin-attached electronics, and alternative materials and geometries are necessary. Hence, various methods have been proposed to provide stretchability to electronic materials, including strain engineering for non-stretchable electronic materials, molecular engineering for intrinsically stretchable materials, and composite engineering for hybrid materials.<sup>[2]</sup> Self-healing ability is essential for recovering functionalities after physical damage of living things. Self-healing materials have been developed through extrinsic and intrinsic approaches.<sup>[21]</sup> Extrinsic self-healing approaches use a composite of healing agents and a matrix material. When a material is damaged, the healing agent spills and chemically reacts with the damaged region to repair it. Intrinsically self-healing materials can heal themselves through intrinsic dynamic molecular interactions, which enables repeatable and reliable self-healing.<sup>[29]</sup> Breathability is another crucial functionality in bio-integrated devices, as it plays a vital role in managing the accumulation of skin by-products that can impede correct sensing from the body and restrict stable adhesion at the

## 1. Introduction

Developments in science and technology have led to the evolution of device form factors, impacting all aspects of our lives. Currently, we are at the forefront of the emergence of new device

J. Y. Oh  
Department of Chemical Engineering (Integrated Engineering Program)  
Kyung Hee University  
Yongin 17104, Republic of Korea  
E-mail: [jyoh@khu.ac.kr](mailto:jyoh@khu.ac.kr)

Y. Lee  
Department of Brain and Cognitive Science  
Korea Advanced Institute of Science and Technology (KAIST)  
Daejeon 34141, Republic of Korea

T.-W. Lee  
Department of Materials Science and Engineering  
Seoul National University  
Seoul 08826, Republic of Korea  
E-mail: [twlees@snu.ac.kr](mailto:twlees@snu.ac.kr)

T.-W. Lee  
Institute of Engineering Research  
Research Institute of Advanced Materials  
Molecular Foundry  
Seoul National University  
Seoul 08826, Republic of Korea  
T.-W. Lee  
School of Chemical and Biological Engineering  
Seoul National University  
Seoul 08826, Republic of Korea

 The ORCID identification number(s) for the author(s) of this article can be found under <https://doi.org/10.1002/adhm.202303797>

DOI: 10.1002/adhm.202303797

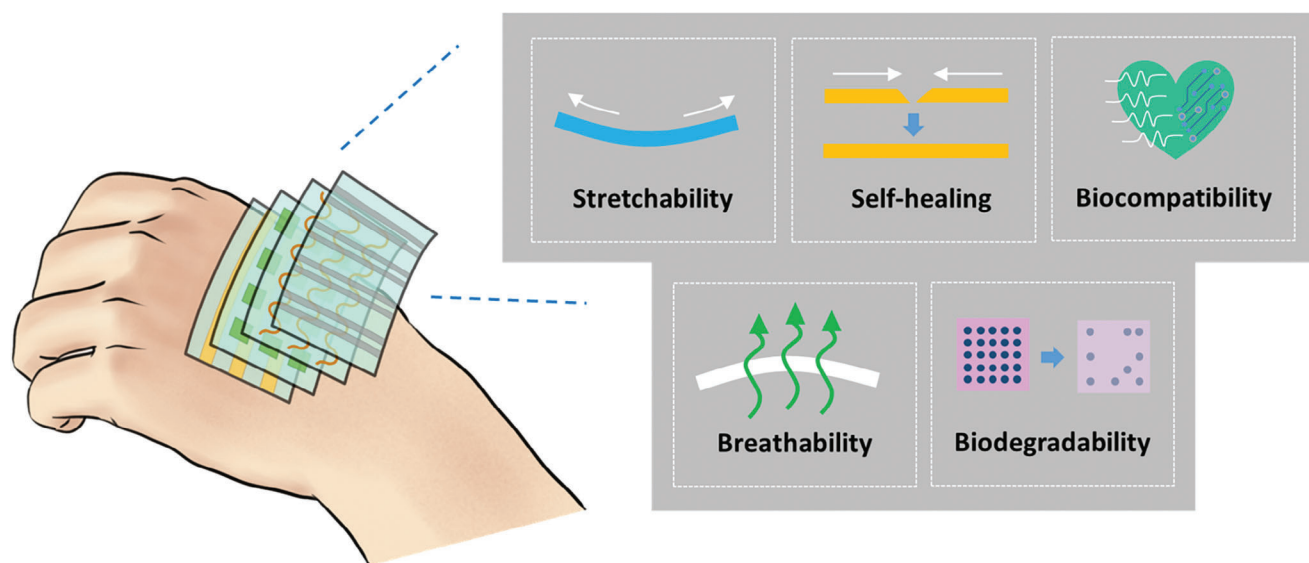


**Figure 1.** Representative functionalities (stretchability, self-healing ability, biocompatibility, breathability, and biodegradability) for skin-mountable functional materials.

interface between the skin and the device. The usefulness of bio-integrated devices has evolved significantly with the implementation of geometrically porous structures that facilitate the transmission of by-products between skin and the environment.<sup>[30]</sup> Biodegradability becomes more important when a device is implanted in the body and discarded naturally without severe surgery for extraction in the end. Various chemical reactions have been applied to functional materials to make them bioresorbable after the device has served its function. Moreover, biodegradability might be a solution to reduce the amount of electronic waste.<sup>[31,32]</sup>

In this perspective article, we discuss recent progress in the development of skin-mountable functional materials, with a focus on these five main functionalities, and identify the current challenges in the adaptation of materials for practical applications. Finally, we conclude with an outlook on the future development of functional materials for bio-integrated skin devices.

## 2. Stretchability

Stretchability refers to the ability of the skin-mountable electronic materials to undergo significant deformation, typically stretching, without losing their electrical properties.<sup>[33–36]</sup> This functionality is essential for creating bio-integrated devices that can conform to the dynamic and complex contours of the human body or other surfaces, thereby enhancing their practicality and comfort in real-world applications.<sup>[37–40]</sup> Stretchable electronic materials can be categorized into conductor, semiconductor, and dielectric materials.<sup>[11,15,41–43]</sup> In this section, we mainly highlight recent progress on stretchable semiconductors in stretchable field-effect transistors integrated with stretchable conducting and dielectric materials, which are essential components of bio-integrated devices.

### 2.1. Stretchable Semiconducting Materials with Macro- and Micro-Scale Modulation

In the initial phase of the development of stretchable electronic materials, structural (or geometrical) stretchability was intensively adopted to conventional rigid electronic materials.<sup>[44,45]</sup> Designing wavy (or serpentine) patterns that utilize strain engineering is an effective method to provide structural stretchability to rigid electronic materials that have been developed over the past few decades and exhibit excellent electrical characteristics.<sup>[46,47]</sup> Recently, this approach has been applied to scalable nanoscale polymer electronics. One option is to use serpentine semiconducting polymer nanowires (SPNWs) for fully stretchable organic field-effect transistors (Figure 2a).<sup>[48]</sup> The electrospun SPNWs were molecularly aligned along the length of the wire by the shear force of the electrospinning extrusion; As a result, intramolecular charge transport was promoted along the aligned SPNWs. Electrospun SPNWs composed of diketopyrrolopyrrole (DPP) semiconductors and polyethylene oxide binders exhibit extreme flexibility and even intrinsic stretchability. To increase the mechanical reliability during strain, the SPNWs were deposited on a pre-strained stretchable substrate to form a serpentine SPNW structure after the pre-strain was released. Serpentine SPNWs have additional structural stretchability, enabling the assembly to retain field-effect mobility after stretching up to 100%. The stretchable SPNW transistor showed highly stable electrical properties during uniaxial strain up to 100% strain and even on a dynamic surface that mimics the 3D expansion during a heartbeat (Figure 2b–d). This approach has been applied to stretchable organic optoelectronic sensor-motor synapses and low-power stretchable neuromorphic nerve systems.<sup>[49,50]</sup>

The molecular blending of semiconducting polymers (SPs) and elastomers can provide intrinsic stretchability to non-stretchable SPs through the nanoconfinement effect

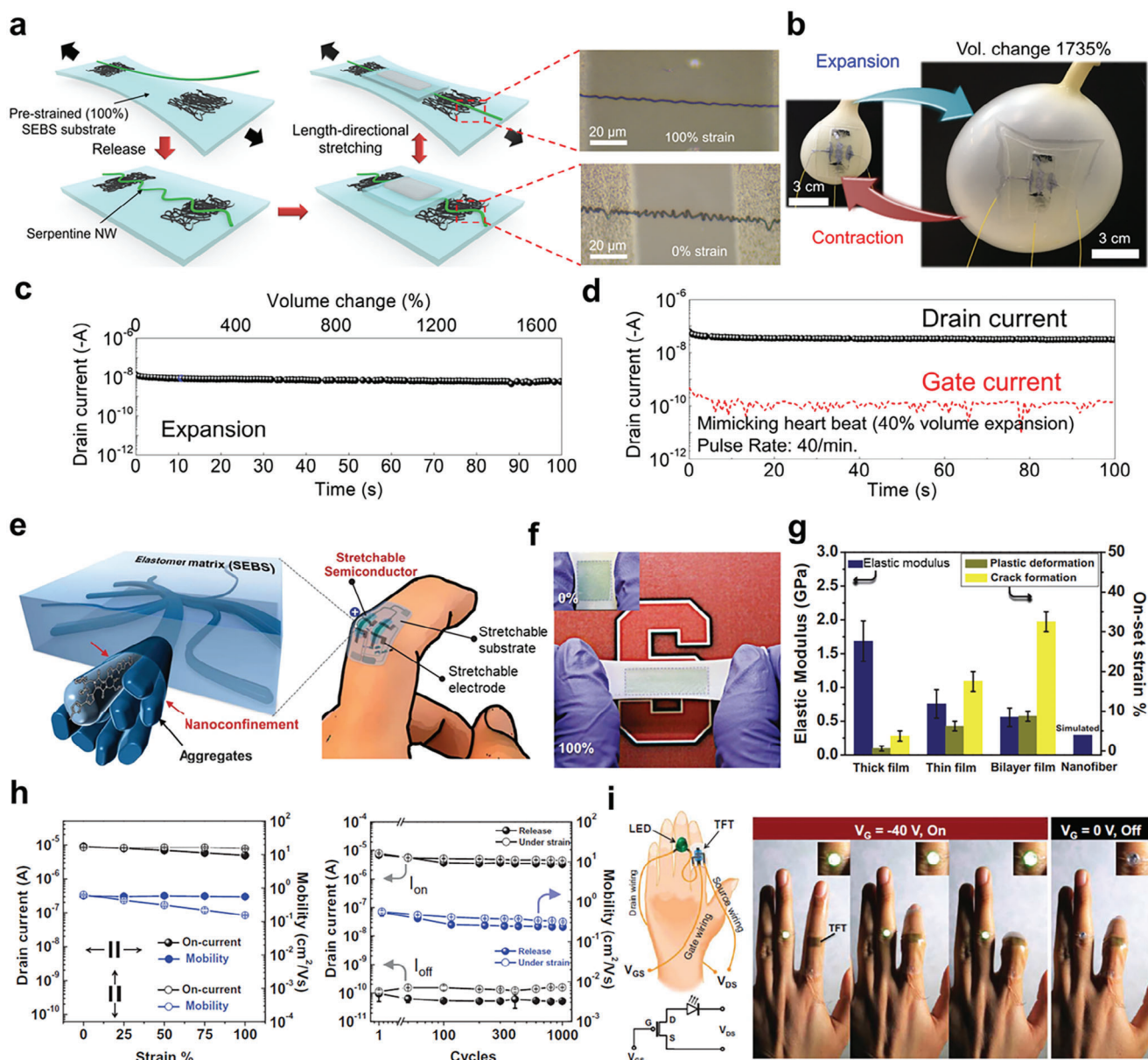


**Figure 2.** Stretchable semiconducting materials with macro- and micro-scale modulation. a) Schematic of fabrication and optical microscope images of a stretchable transistor with serpentine semiconducting polymer nanowire (SPNW) before and after 100% stretching. b) A stretchable SPNW transistor attached to the surface of a dynamic balloon that emulates a beating heart. c) Drain current of stretchable SPNW on the balloon during >1700% volume expansion. d) Drain and gate current of stretchable SPNW on a dynamic balloon. Reproduced with permission.<sup>[48]</sup> Copyright 2018, Wiley-VCH. e) Schematic of nanoconfined polymer semiconductor fibril networks embedded in the elastomer matrix. f) Photographs of nanoconfined stretchable polymer semiconducting film before and after 100% stretching. g) Elastic moduli and onset strains of crack formation and plastic deformation of nanoconfined stretchable polymer semiconducting films (upper right). h) Changes of the on-current and carrier mobility in both parallel (left) and perpendicular (right) directions with strains up to 100% (left). Changes of the on-current, off-current, and carrier mobility after 1000 stretching cycles at 25% strain along the parallel direction (right). i) Demonstration of a finger-wearable stretchable transistor for LED operation. Reproduced with permission.<sup>[51]</sup> Copyright 2017, American Association for the Advancement of Science.

(Figure 2f).<sup>[51]</sup> The nanoconfinement effect amplifies the polymer chain dynamics in the nanoconfined structure, which significantly reduces both the glass transition temperature and Young's modulus of the SP in the elastomer matrix, thus making the SPs intrinsically stretchable in nanoconfined dimensions (Figure 2g). The blended film could be stretched up

to 100% strain without sacrificing charge-transport mobility (Figure 2h). The film was used to demonstrate a skin-like wearable device that uses fully stretchable transistors to power a light-emitting diode. It has been widely applied to various stretchable electronic devices and further developed for skin electronics (Figure 2i).<sup>[51–53]</sup>

## 2.2. Stretchable Semiconducting Materials with Molecular-Scale Modulation

The intermolecular crosslinking of SPs using elastomeric crosslinkers is a systematic method that provides elasticity to non-elastic SPs via a chemical reaction for stretchable semiconducting films (Figure 3a).<sup>[54]</sup> One method uses chemical crosslinking via hydrosilylation to produce an elastically stretchable semiconductor.<sup>[54]</sup> SPs derived from DPP were crosslinked using a siloxane crosslinker via a hydrosilylation reaction with reactive side chains, which provided mechanical elasticity to the SP. This elasticity was controlled by the content of the reactive side chains, and the cross-linked semiconducting film did not redissolve. A polymer semiconductor reacting with 20% elastomer crosslinker can be stretched >100% without mechanical damage (Figure 3b,c).<sup>[54]</sup>

The incorporation of intermolecular dynamic bonds into SP is a multifunctional strategy that provides both intrinsic stretchability and self-healing ability to SP. The first report of an intrinsically stretchable self-healing SP utilized hydrogen bonding (Figure 3d).<sup>[55]</sup> A pyridinedicarbozamine (PDCA) moiety capable of hydrogen bonding was incorporated into the backbone of the DPP-derived SP. When a polymer is stretched, hydrogen bonds can easily break and spontaneously reform; therefore, the main backbone does not break permanently. The reversible rupture of hydrogen bonds also provides an energy dissipation mechanism. Appropriate control of the content of non-conjugated PDCA units in the polymer backbone maximizes the intrinsic stretchability without a significant loss of electrical properties (Figure 3e). In addition, the SP film healed after mechanical damage. Nanocracks caused by fatigue failure in the semiconducting film can be healed by exposing it to solvent vapor to achieve recontact, followed by thermal treatment to reorganize the film morphology (Figures 3f,g).<sup>[55]</sup>

## 2.3. Stretchable Conductors and Dielectric Materials

Stretchable electrodes are essential components of stretchable transistors. Carbon nanotubes (CNTs) are widely used as stretchable electrodes because of their moderate stretchability and conductivity. However, uniform deposition of CNTs on large-area substrates needs improvement to achieve reliable characteristics of device array.<sup>[56–58]</sup> In contrast, metal is an ideal conductor with high conductivity and capability of uniform deposition on large-area substrate. However, it is difficult to make it soft and elastic. Recently, Kim et al. presented a creative method for fabricating a silver (Ag) stretchable electrode through metal-polymer intermixing for transistors (Figure 4a).<sup>[59]</sup> They utilized vaporized Ag atoms interfused with an elastic polymer semiconducting film. Ag has a higher surface diffusivity than other noble metals, such as gold and copper, allowing it to efficiently diffuse into an elastic semiconductor matrix, forming a metal-polymer nanocomposite (Figure 4b). The metal-polymer nanocomposite layer has versatile functions for stretchable electrodes: E.g., the nanocomposite acted as a physical glue at the interface Ag electrode/semiconductor layers, which made the Ag electrode stretchable up to 100% uniaxial strain (30% biaxial strain) without significant changes in conductivity ( $>10^4$  S/cm) (Figure 4c,d).

Even after several peel-off tests using the 3 M adhesive tape, its morphology and electrical properties were almost completely preserved. Moreover, the high work function of  $\text{Ag}_2\text{O}$  (5.2 eV) created on the Ag nanoclusters by surface oxidation forms an ohmic contact with semiconductors for efficient current injection, enabling the fabrication of a strain-insensitive active-matrix transistor array for skin electronics.

Dielectrics is one of the key materials in terms of the low operation voltage of transistors. Most reported stretchable transistors have been fabricated with conventional elastomer dielectrics such as polydimethylsiloxane (PDMS) and styrene-ethylene-butylene-styrene (SEBS), which have high intrinsic stretchability and dielectric strength without ionic impurities; However, the low dielectric constant ( $\kappa$ , 2–3) and high thickness ( $>1$   $\mu\text{m}$ ) of conventional elastomers induce a relatively low capacitance compared to rigid inorganic and oxide materials at the same applied voltage. This makes it difficult to accumulate charge carriers for active channel formation, increasing the operating voltage of the device.<sup>[48,52,60]</sup> Consequently, the development of high-dielectric materials or a reduction in the thickness of the dielectric is required to achieve a low operating voltage. Recently, Koo et al. fabricated an ultrathin elastic dielectric using the vacuum deposition process (Figure 4e).<sup>[61]</sup> They proposed the initiated chemical vacuum deposition (iCVD) method for the copolymerization and crosslinking of two monomers: isononyl acrylate (INA) as the soft primer and 1,3,5-trimethyl-1,3,5-trivinyl cyclotrisiloxane (V3D3) as a crosslinkable hard segment, which provided robust insulator performance to ultrathin films (200 nm) (Figure 4f). Stretchable transistors made of the iCVD-based elastic dielectric showed a performance comparable to transistors with a traditional oxide dielectric (aluminum oxide,  $\text{Al}_2\text{O}_3$ ) and high dielectric uniformity on an 8-inch wafer (Figure 4g).

## 2.4. High-Resolution Direct Photopatterning of Stretchable Materials for High-Density Transistors

Although remarkable progress has been made in the development of various stretchable electronic materials, the absence of a scalable fabrication technology for stretchable transistors with reported stretchable semiconductors has restricted the advancement of skin electronics. Direct photopatterning based on selective photocrosslinking chemistry can provide fast and scalable fabrication of multiple functional layers stacked for high-resolution and high-density transistor arrays on large-area. Wang et al. introduced a photopatterning method based on azide crosslinking chemistry for polymer electronic materials consisting of stretchable transistor arrays (Figure 5a).<sup>[52]</sup> The key technology of this method is the patterning of the elastomer dielectric via UV photocrosslinking reaction of the azide group of the crosslinker and the alkyl group of the elastomer dielectric, which enables stacking of the semiconducting layer and electrodes on the photocrosslinked elastomer dielectric with solvent resistance (Figure 5b,c). The patterned transistor array with 347 transistors/ $\text{cm}^2$  shows highly uniform field effect mobility comparable to that of an amorphous silicon transistor, even under 100% tensile strain. They demonstrated active matrix sensor arrays and analog and digital circuit elements, such as a pseudo-CMOS, a NAND gate, and a signal amplifier (Figure 5d).

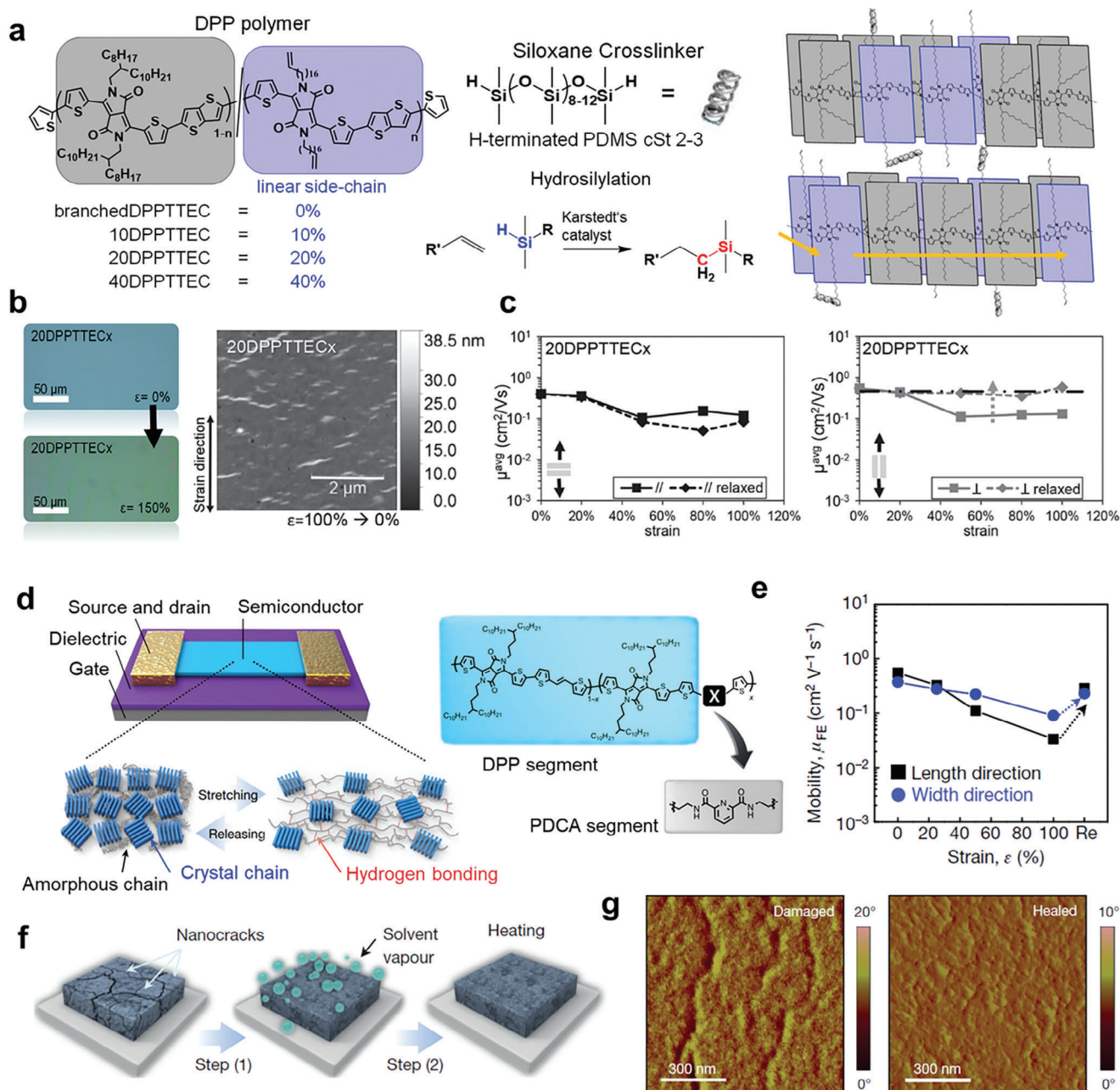


**Figure 3.** Stretchable semiconducting materials with molecular-scale modulation. a) Chemical structures of intrinsically stretchable polymer semiconductors that have hydrosilylation reaction, which is intermolecular chemical crosslinking between DPP-derived polymer and siloxane crosslinker (H-terminated PDMS crosslinkers) (left). Schematic of molecular packing in the covalently crosslinked stretchable SP film (right). b) Optical microscope images of the crosslinked SP film with 20% linear side chain (20DPPPTTECx) before and after 150% stretching (left) and an AFM image of the released 20DPPPTTECx after 100% strain (right). c) Change in carrier mobility of stretched 20DPPPTTECx film in the soft-contact lamination OTFT under various strains in parallel and perpendicular directions. Reproduced with permission.<sup>[54]</sup> Copyright 2016, Wiley-VCH. d) Schematic of a polymer transistor with an intrinsically stretchable DPP-derived polymer semiconductor film that incorporates non-conjugated PDCA moieties for intermolecular dynamic hydrogen bonding units (left). Chemical structures of the DPP segment and the PDCA segment (right). e) Carrier mobility of skin-mountable intrinsically stretchable transistors under various strains in the channel length and width directions. f) Schematic of healing process of damaged semiconducting film that has nanocracks with solvent vapor and heating treatments. g) AFM images of damaged and healed semiconducting film. Reproduced with permission.<sup>[55]</sup> Copyright 2016, Springer Nature.

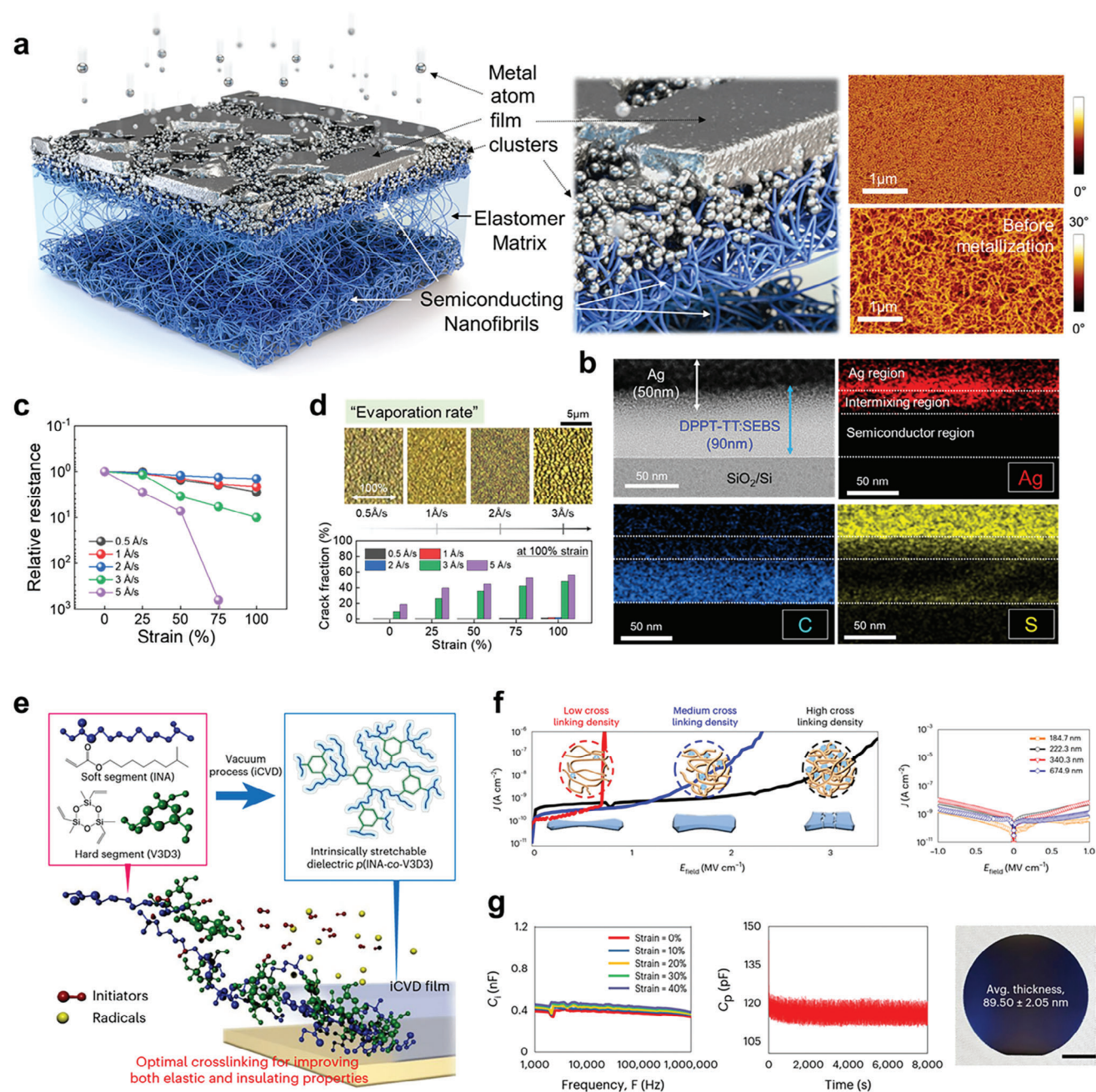


**Figure 4.** Stretchable conductors and dielectric materials. a) Schematic illustration of stretchable metallization (left) and the AFM images before and after metallization on elastic semiconducting polymer film (right). b) Cross-sectional transmission electron microscope images and energy-dispersive X-ray spectroscopy mapping images for Ag, C, and S atoms. c) Resistance change of Ag-metallized films with various deposition rates under strain. d) Optical microscope images (top) and crack fraction (bottom) of Ag-metallized films with different deposition rates after 100% stretching. Copyright 2023, American Association for the Advancement of Science.<sup>[59]</sup> e) Schematic of the iCVD process for depositing the stretchable polymer dielectric using INA and V3D3 monomers. f) Current density-electric field characteristics of stretchable dielectrics with various monomer compositions (left) and a plot of the capacitance of p1V1 (C<sub>p</sub>) as a function of time during 1000 cyclic stretching with 40% strain (right). g) Capacitance-frequency curves of MIM devices with p1V1 dielectric under various strains (left), a plot of the capacitance of p1V1 (C<sub>p</sub>) as a function of time during 1000 cyclic stretching with 40% strain (middle), and large-area uniformity of the stretchable dielectric deposited on an 8-inch wafer. Reproduced with permission.<sup>[61]</sup> Copyright 2023, Springer Nature.

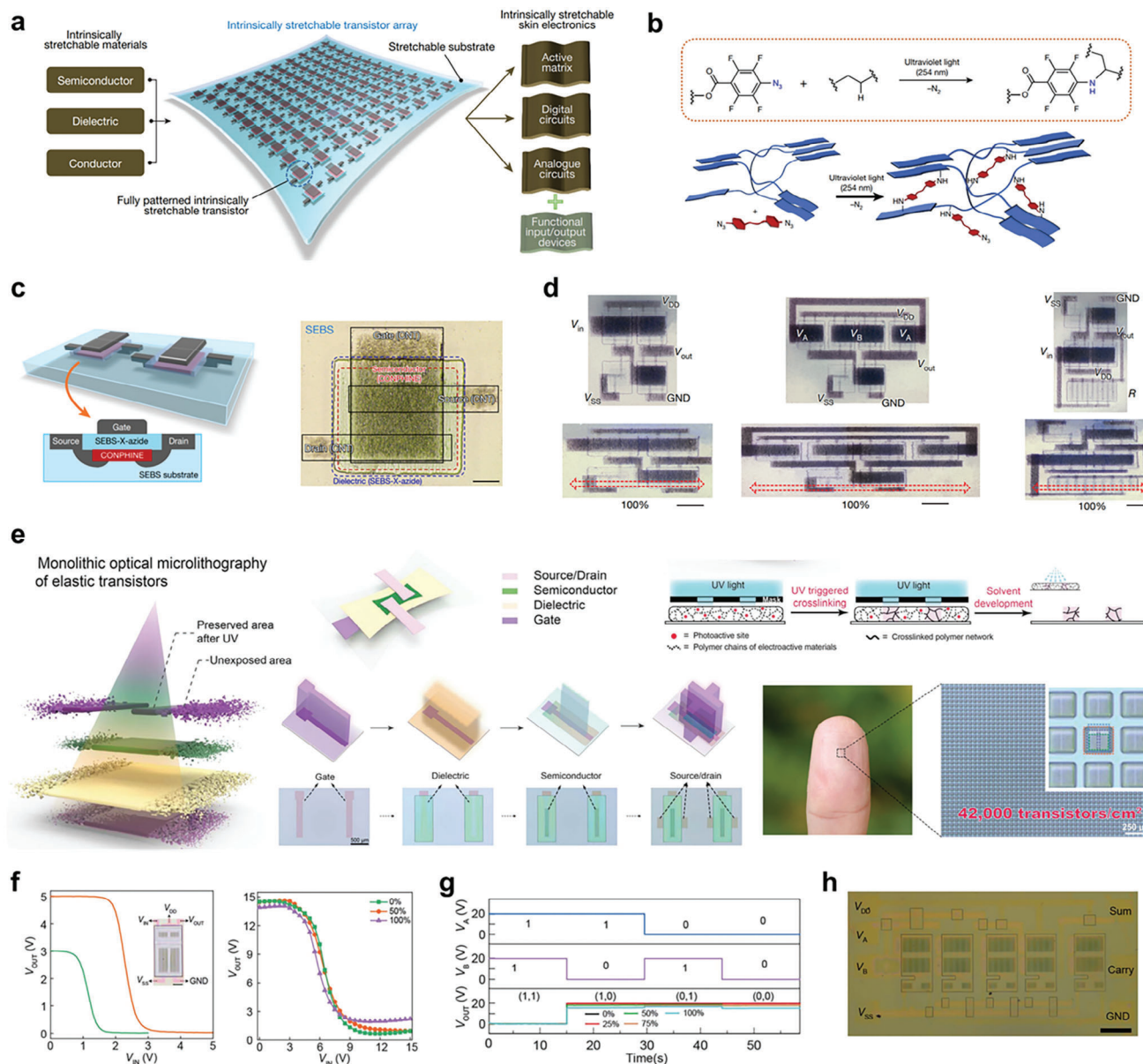


**Figure 5.** High-resolution direct photopatterning of stretchable materials for high-density transistors. a) Schematic of an intrinsically stretchable transistor array as the core building block of skin electronics. b) Mechanism of the azide-crosslinking reaction, which is initiated by UV light and is based on the reaction between azide groups and CH groups. c) Schematic and optical microscope images of an intrinsically stretchable pseudo-CMOS inverter (left), NAND gate (middle), and amplifier (right). Reproduced with permission.<sup>[52]</sup> Copyright 2018, Springer Nature. e) Schematic illustration of monolithic optical microlithography (left), elastic electronic materials are directly patterned sequentially by a series of UV light-triggered solubility modulation processes (middle), and an elastic transistor array containing 10 000 transistors attached seamlessly onto the finger (right). f) Transfer characteristics of the pseudo-D 10- $\mu\text{m}$  inverter (left) and transfer characteristics of the pseudo-E 50- $\mu\text{m}$  inverter under strain (right). g) Output characteristics of the pseudo-E 50- $\mu\text{m}$  NAND gate under strain. h) Optical microscope image of a half-adder consisting of 30 transistors. Reproduced with permission.<sup>[62]</sup> Copyright 2021, American Association for the Advancement of Science.

This study demonstrates the high potential for the scalable fabrication of stretchable electronic devices. Moreover, a delicate method, such as photolithography, which is a core technology of the semiconductor industry, to reduce the device scale to submicrometers is also necessary in developing skin electronics.

Recently, Zheng et al. reported an advanced photopatterning method for the microlithography of high-density stretchable devices.<sup>[62]</sup> They achieved the direct optical patterning of mul-

tipple electroactive materials (conductors, semiconductors, and dielectrics) through exposure to UV light (Figure 5e). Semiconductor and dielectric materials were directly patterned using the light-triggered carbene region of the crosslinker, and the conducting polymer was patterned for the source/drain and gate electrodes using dual-network-mediated optical lithography. This approach takes advantage of both the post-functionalization properties of polymer electronic materials and conventional

photolithography for high-density devices without using photoresist or stripping processes, which limit the applications of photolithography to stretchable polymer materials.<sup>[63,64]</sup> They achieved a maximum density of elastic stretchable transistors of up to 43200/cm<sup>2</sup> and fabricated elastic functional devices (XOR gates and half-adders) consisting of elastic transistors, which are the fundamental components of an arithmetic logic unit.

Poly(3,4-ethylenedioxythiophene)-poly(styrenesulfonate) (PEDOT:PSS) is also one of the most promising stretchable electrodes due to its intrinsic flexibility and high work function (>5.0 eV). An elastic and patternable PEDOT:PSS electrode was developed using a photocrosslinking method.<sup>[62,65]</sup> PEDOT:PSS crosslinked with a polyethylene glycol dimethacrylate (PEGDMA) crosslinker has mechanical elasticity, and the fiber-like conducting PEDOT network significantly increases its electrical conductivity (>5000 S cm<sup>-1</sup>); However, the inherent instability of conducting polymers in air and their relatively low electrical conductivity remain challenges.

The perspective on stretchability in electronic materials for bio-integrated devices aims to advance the field of materials science by creating highly adaptable and durable materials. These materials can possess diverse functionalities such as self-healing, biocompatibility, and biodegradability, making them indispensable for the development of future bio-integrated skin devices. These advancements hold significant importance for the next generation of wearable electronics and flexible devices, unlocking vast potential across various applications, ranging from personal healthcare to interactive technology.

### 3. Self-Healing

#### 3.1. Extrinsic and Intrinsic Self-Healing Materials

Self-healing ability has been regarded as an exclusive property of living things, and smart electronic materials have recently adopted this healing ability to prevent mechanical damage.<sup>[66,67]</sup> This functionality aims to mimic the regenerative abilities of human skin, thereby enhancing the durability and functionality of electronic devices that are designed to be skin-integrated devices. The self-healing materials have been developed by extrinsic and intrinsic self-healing mechanisms involving strain engineering and material chemistry, respectively. The extrinsic self-healing ability was first introduced using healing agents such as microcapsules and vessels embedded in conventional polymers (Figure 6a).<sup>[68–71]</sup> When a material is physically damaged, the microcapsules break and release healing agents, which then begin to fill the damaged regions of the polymers and chemically crosslink with each other to heal the damage (Figure 6b). Recently, liquid metal (LM) microcapsule-based elastomer composites have been widely applied for autonomously electrical healing conductors.<sup>[72,73]</sup> The LM microcapsules have demonstrated a remarkable capability to efficiently restore electrical functionality in mechanically damaged composites, especially compared to solid-based conducting fillers. This achievement is realized through the rapid and adaptive rupture of the LM microcapsules around the damaged regions. This advancement has facilitated the development of bio-inspired self-healing conductive materials. The extrinsic self-healing method has a simple working mechanism and can be easily applied to traditional polymer ma-

terials; However, it is not repeatable, and the chemical reaction for self-healing is difficult to control.

Intrinsic self-healing does not require external healing agents and therefore avoids these drawbacks.<sup>[21]</sup> Dynamic intermolecular interactions, i.e., dynamic bonds such as hydrogen bonds, metal coordination, and electrostatic interactions, provide the key driving force for intrinsic self-healing.<sup>[74,75]</sup> The dynamic bonds can easily break and undergo spontaneous reformation to achieve self-healing properties.<sup>[76,77]</sup> For example, the dual dynamic bond system uses weak and strong crosslinking hydrogen bonds and can efficiently self-heal via reversible hydrogen bond formation and mechanical elasticity in the polydimethylsiloxane (PDMS) backbone. As a result, this self-healing elastomer had high toughness (12000 J m<sup>-2</sup>), stretchability (without notch: 3000%, with notch: 1200%), and transparency (98%) (Figure 6c,d). This self-healing elastomer is not sensitive to water, which may facilitate its application in bio-integrated electronic devices (Figure 6e,f).<sup>[77]</sup>

#### 3.2. Functional Self-Healing Materials

With the development of multidynamic bond systems, self-healing polymers have been further developed by mimicking muscle behavior.<sup>[78,79]</sup> A mechanoresponsive self-growing hydrogel has polymer chains that can be mechanically reinforced after an external strain breaks the first network, which consists of rigid and brittle covalent bonds (Figure 7a).<sup>[78]</sup> When the hydrogel is damaged by an external strain, the broken chains generate mechanical groups that react with the monomers, thereby reinforcing the mechanical properties by reconstructing the hydrogel networks, similar to muscle building (Figure 7b). This mechanoresponsive hydrogel, inspired by muscle training, facilitates force-initiated reactions that control the mechanical properties of self-healing polymers at the molecular level.<sup>[78]</sup>

One potential approach to providing conducting or semiconducting properties to insulating self-healing materials is combining self-healing polymers with CPs, thereby expanding their applications to bio-integrated self-healing semiconductor devices.<sup>[60]</sup> A rational strategy for combining self-healing materials and conjugated polymers was developed using dynamic crosslinking.<sup>[60]</sup> The dynamic molecular crosslinking strategy utilizes the metal coordination of these materials to achieve an intrinsically self-healing semiconducting film (Figure 7c). Both SP and self-healing elastomers have the same dynamic bond unit (PDCA) in their backbones, which forms a dynamically crosslinkable metal-ligand coordination complex via Fe(III)-PDCA coordination. The Fe(III)-PDCA coordination chemistry has three different dynamic bonds (Fe-N<sub>pyridyl</sub>, strong; Fe-N<sub>amido</sub>, medium; and Fe-O<sub>amido</sub>, weak), which together enable dynamic cross-linking for intrinsic stretchability and self-healing (Figure 7d). The morphology of the combined film was controlled by adjusting the polymer blend ratio to obtain a strain-sensitive self-healing semiconductor for e-skin sensor applications (Figure 7e).<sup>[60]</sup>

Most self-healing tests have been conducted using a single layer; However, complex electronic devices consist of multifunctional layers. E.g., a transistor can be stacked using a combination of gate/dielectric/semiconductor/source-drain electrode layers. Thus, self-alignment of the damaged multilayers of electronic devices is essential for the restoration of functionality after self-



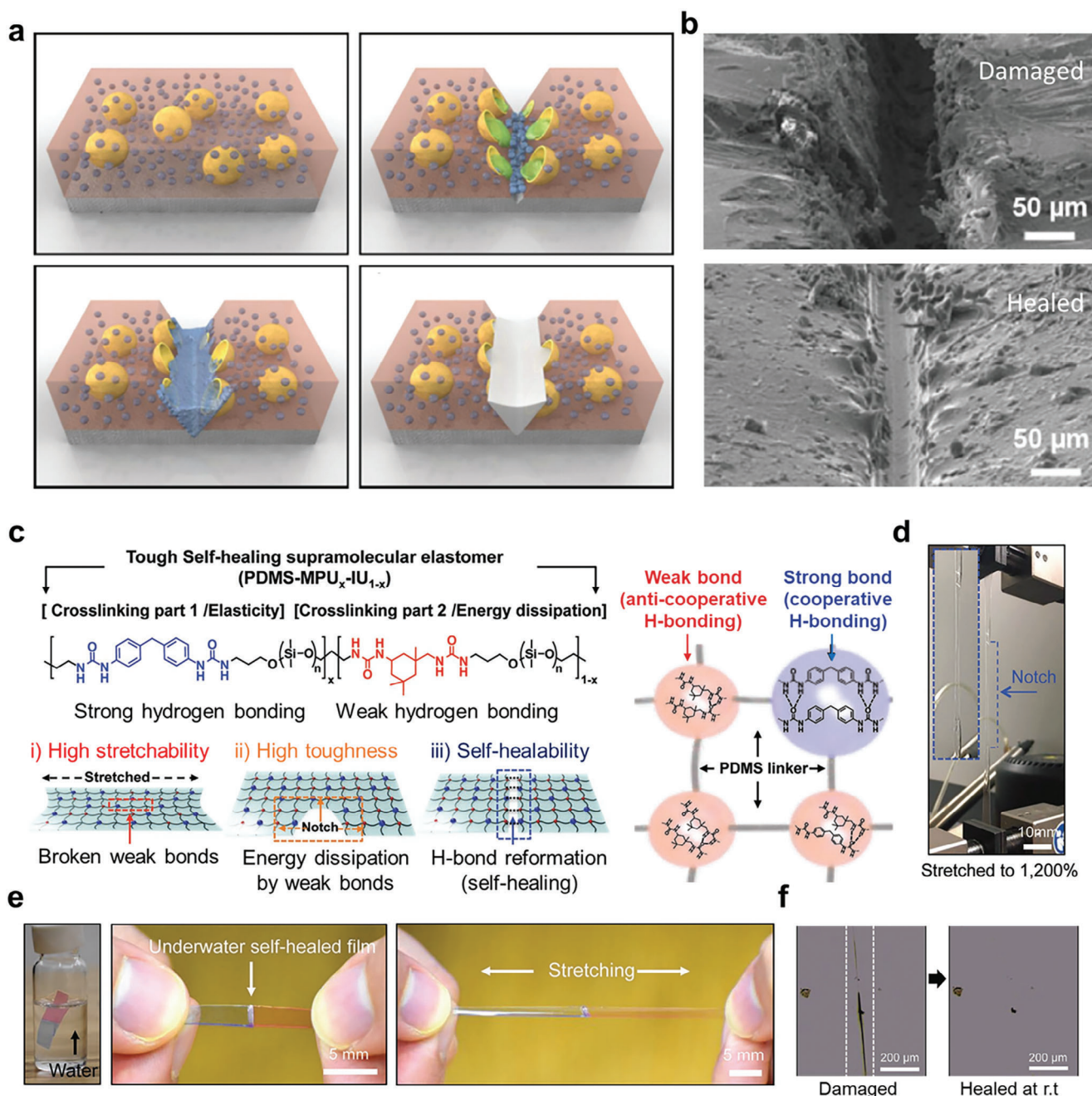


**Figure 6.** Extrinsic and intrinsic self-healing materials. a) Schematics of the self-healing mechanism of the extrinsic self-healing material with microcapsules. The healing agent and catalyst are mixed in the damaged region. b) Scanning electron microscope images of the damaged metal substrate without and with a self-healing coating layer. Reproduced with permission.<sup>[68]</sup> Copyright 2009, Wiley-VCH. c) Schematics of molecular structures of intrinsic self-healing elastomers with a dual dynamic bond system. d) Photograph of the notched intrinsic self-healing elastomer after 1200% stretching. e) Photographs of intrinsic self-healing elastomer healed in the water before and after stretching and f) optical microscope images of damaged and healed intrinsic self-healing elastomer after heating at room temperature (right). Reproduced with permission.<sup>[77]</sup> Copyright 2018, Wiley-VCH.

healing. Recently, Cooper et al. introduced autonomous alignment and healing in multilayers by using immiscible dynamic polymers.<sup>[80]</sup> They utilized the immiscibility of two different polymer backbones with identical dynamic bonds: polydimethylsiloxane (PDMS) and polypropylene glycol (PPG), with identical dynamic bonds. Although their polymer backbones have low

miscibility, their identical dynamic bonds allow weak interpenetration to maintain interlayer adhesion, preventing the multilayer polymer films from delaminating (Figure 7f). The self-alignment of the damaged multilayers was primarily induced to minimize the interfacial free energy for self-healing, and molecular dynamics simulations supported this mechanism (Figure 7g,h).

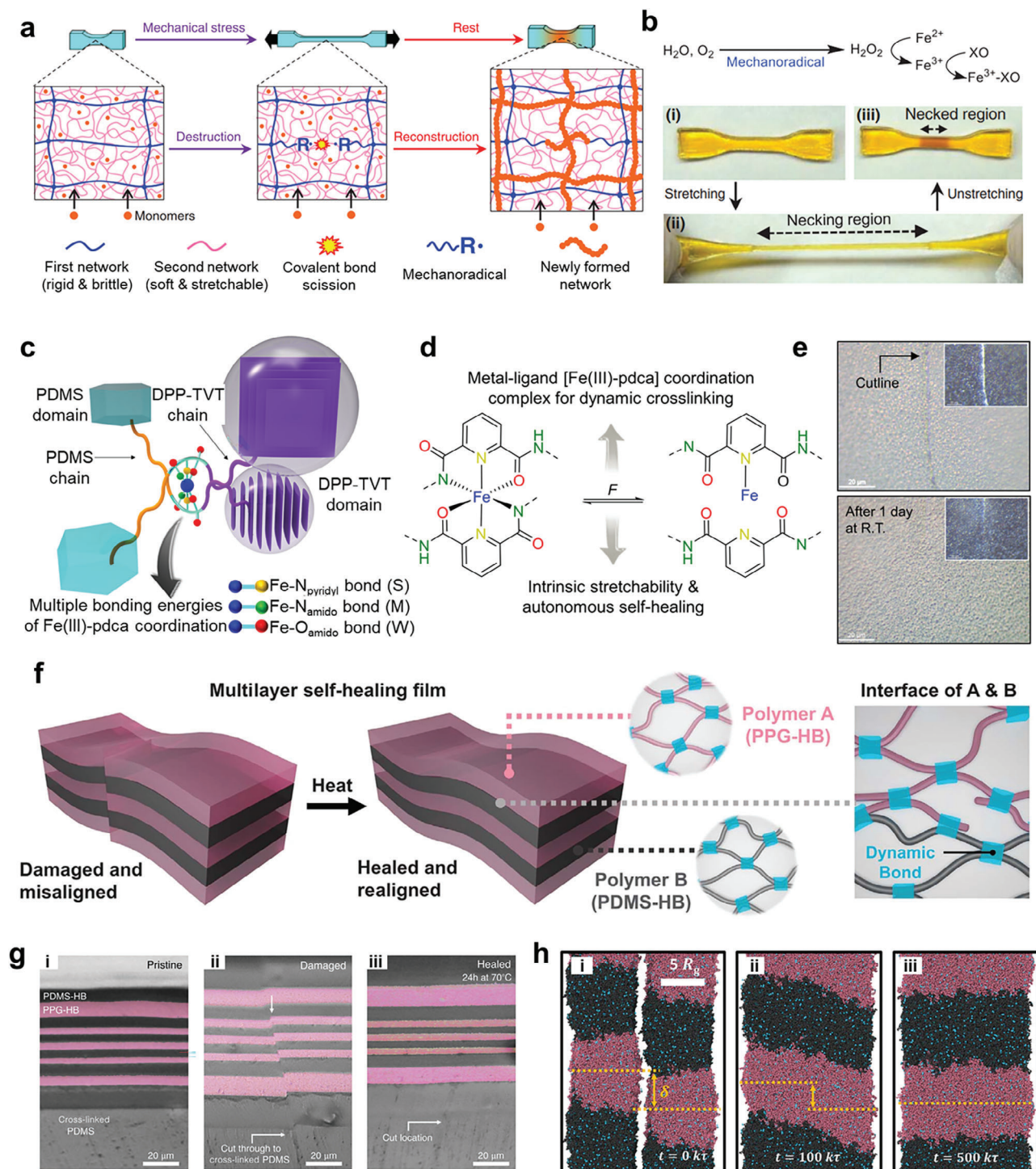


**Figure 7.** Functional self-healing materials. a) Schematics of the molecular structures of a mechanoresponsive self-growing hydrogel. b) Chemical reactions with mechanoradicals ( $\bullet R$ ) and photographs of a mechanoresponsive self-growing hydrogel, (i) before, (ii) during, and (iii) after 350% stretching. Reproduced with permission.<sup>[78]</sup> Copyright 2019, American Association for the Advancement of Science. c) Schematic of molecular structures of self-healing semiconductors in which the elastomer and conjugated polymer are combined by dynamic bonding unit (PDCA) with metal-ligand coordination. d) Chemical structure of the metal-ligand coordination complex for dynamic crosslinking. e) Optical microscope images of a damaged self-healing semiconductor film. Reproduced with permission.<sup>[60]</sup> Copyright 2019, American Association for the Advancement of Science. f) Schematic illustration of the principle of surface tension-mediated realignment and healing of a fractured multilayer. g) Cross-sectional optical microscope images of (i) the pristine hot-pressed multilayer, (ii) the damaged and misaligned laminate, and (iii) the healed and realigned laminate after annealing for 24 h at 70 °C. h) Simulation snapshots showing how an initially misaligned and separated laminate aligns and heals over time. Reproduced with permission.<sup>[80]</sup> Copyright 2023, American Association for the Advancement of Science.

Despite significant progress in the development of self-healing materials, there is still much room for further development. Particularly, self-healing of microscale damages for submicron-thick films, which are the typical thickness range of electronic layers, is important because most areas of damage (scratch, stab, and mark) are  $>1\ \mu\text{m}$  or entail material loss.<sup>[60]</sup> In addition, intrinsically self-healing materials mostly exhibit insulating properties; consequently, self-healing semiconductors and conductors are being developed by mixing them with self-healing insulating materials. The development of intrinsically self-healing semiconductors and conductors will facilitate the development of fully self-healing electronic devices.

## 4. Biocompatibility

Biocompatibility in skin-mountable electronic materials is a critical aspect in the evolving field of wearable technology and bio-integrated devices. To achieve long-term stability during the integration of devices into the human body, they must not cause harm or induce an immune response and must have similar mechanical properties to those of tissues, particularly when the devices are integrated into the body for long-term use.<sup>[10,81–83]</sup> Until now, most biocompatible materials have been developed for wearable and implantable devices with geometrical advantages such as mesh structures to avoid the scarring response to rigid metal electrodes. For better long-term stability, intrinsically biocompatible materials must be developed for integration into the body. Various approaches for improving the biocompatibility of electronic materials have been proposed.<sup>[84–86]</sup>

### 4.1. Biocompatible Polymer Materials

Hydrogels are biocompatible materials with high softness and elasticity.<sup>[87–89]</sup> Hydrogel is especially useful for implantable electronic materials.<sup>[90–92]</sup> Conventional implants have been fabricated using rigid electronic materials, which induce a mechanical mismatch with the tissue of the body and can increase immune responses.<sup>[93–95]</sup> To overcome this problem, hydrogels have been intensively investigated as key materials for biocompatible implants.<sup>[96,97]</sup>

Soft and elastic hydrogel electrodes with a low Young's modulus (of the order of 10 kPa) have been developed for implantable neuromodulation microelectronics (Figure 8a,b).<sup>[96]</sup> Electrically conductive hydrogels (ECH) were prepared using PEDOT:PSS and an ionic liquid via water exchange and hydration processes. Combining the ECH with a photolithographic fluorinated elastomer enables the micropatterning of the ECH electrodes with resolutions as fine as  $5\ \mu\text{m}$  and strain-insensitivity (Figure 8c,d). The micropatterned ECH electrode ( $20\ \mu\text{m}$  in feature size) is strain-insensitive (up to 20%) with lower interfacial impedance and better current injection density than conventional metal electrodes, thus localized low-voltage neuromodulation was achieved (Figure 8e,f).<sup>[96]</sup>

For further miniaturization of bio-integrated devices with better electrical properties, a rational molecular design of conducting polymers is required. Jiang et al. presented a topological supramolecular network-based molecular engineering strategy

that improved the conductivity and mechanical robustness of a conducting polymer with photopatternability down to cellular scale and high stretchability, providing biocompatibility and seamless bio-integration of the device into the human body.<sup>[65]</sup> Figure 8g shows a rationally designed topological supramolecular network system based on PEDOT:PSS, which is a representative conducting polymer for bioelectronic devices, and a newly designed multifunctional supramolecular cross-linker (Figure 8h). It consists of a rotaxane-structured hydrophilic backbone for the removal of PSS and the reduction of PEDOT crystallinity, with a water-soluble and crosslinkable side chain for the photopatterning of the conducting polymer. The crosslinked PEDOT:PSS based on a topological supramolecular network was highly stretchable, allowing it to maintain its improved conductivity, and photopatternability for biocompatible soft electrodes (Figure 8i). With these advantages, a stretchable high-density electrode was fabricated using direct photopatterning, which enabled precise localized neuromodulation for the accurate control of individual muscle activities (Figures 8j–l).

### 4.2. Injectable Biocompatible Materials

To achieve stable, long-term, and continuous monitoring of body signals when electronic components are integrated into the body, they should be capable of seamless and minimally invasive 3D interpenetration with tissues.<sup>[98,99]</sup> One strategy for loading electronic components into biological structures is to use a syringe to inject a mesh structure containing electronic components with submicron-scale thickness and centimeter-scale area (Figure 9a).<sup>[98]</sup> The injected nanomesh electronics spontaneously unfolded with 90% device yield by covering nonplanar biological structures (Figure 9b). Although mesh electronics consist of conventional metal, silicone, and polymer materials, syringe-injected mesh electronics have unique biocompatibility owing to their ultra-small bending stiffness and micrometer-scale features compared to thin-film electronics. These geometrical advantages of syringe-injectable mesh electronics enabled *in vivo* stereotaxic injection of mesh electronics into the mouse brain and *in vivo* recording of 16-channel signals from the brain (Figure 9c,d).<sup>[98]</sup>

*In vivo* polymerization of conducting polymers in living cells has recently been introduced as an alternative to injection for neurotargeted electrical modulation.<sup>[100]</sup> The method uses complex cellular architectures with genetically encoded enzymes and conjugated polymer precursors (Figure 9e). Polymer precursors can be polymerized using encoded enzymes in the plasma membrane of genetically targeted cells. CPs that are directly synthesized on genetically targeted cells can be electrically functionalized as conductors or insulators for efficient electrical neuromodulation of living cells (Figure 9f). This approach could maximize the therapeutic effects of electric neuromodulation while minimizing undesired side effects compared with conventional approaches, such as pharmacology or bioelectric medicine, that use rigid microneedles or flexible cuff electrodes (Figure 9g).<sup>[101]</sup>

The biocompatibility of electronic materials is continuously evolving with the development of new materials and technologies. Current challenges include creating more robust, long-lasting materials that maintain biocompatibility over time

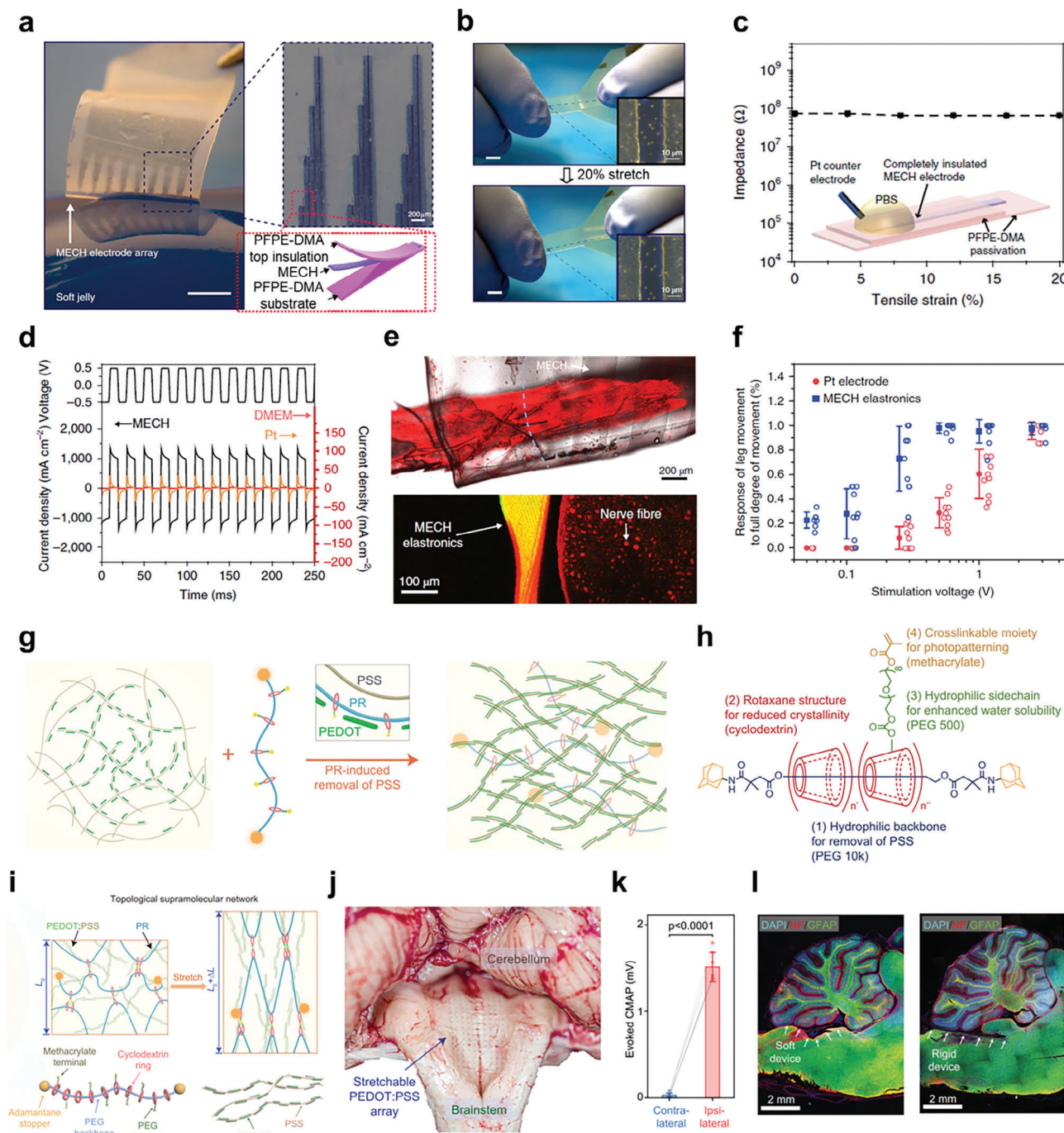


**Figure 8.** Biocompatible polymer materials. a) Photograph and optical microscope images and schematic of the biocompatible micropatterned electrically conductive hydrogel (MECH) electrode array. b) Photograph and optical microscope images of the MECH electrode array before and under 20% tensile strain. c) Change in impedance of encapsulated MECH electrodes by Perfluoropolyether dimethacrylate (PFPE-DMA) at 1 kHz under different strains. d) Current densities of different electrodes (electronic conductor platinum, ionic conductor Dulbecco's Modified Essential Medium (DMEM), and electric-ionic dual conductor MECH) measured at a frequency of 50 Hz. e) Confocal microscope image of MECH electrodes on an elastic substrate that conformably wraps around a sciatic nerve. f) The leg movement (%) with different amplitudes of stimulation voltage for the conventional Pt and MECH electrodes. Reproduced with permission.<sup>[96]</sup> Copyright 2019, Springer Nature. g) Schematic illustration and h) chemical structure of polyrotaxane (PR)-polyethylene glycol methacrylate (PEGMA) interacting with PEDOT:PSS. i) Schematic illustration of intrinsically stretchable PEDOT:PSS with a topological supramolecular network with the key moieties of PR monomers (L: length of film). j) Photograph of a stretchable PEDOT:PSS array conformably attached to the brainstem. k) Statistical analyses of the preferred activation of ipsilateral targets (CMAP: compound muscle action potential). (l) Brain slice immunohistological staining after the insertion of the soft and stretchable electrode array (left) and a rigid device (right) along the floor of the fourth ventricle between the brainstem and the cerebellum (DAPI: 4',6-diamidino-2-phenylindole, NF: neurofilament, GFAP: glial fibrillary acidic protein). Reproduced with permission.<sup>[65]</sup> Copyright 2022, American Association for the Advancement of Science.

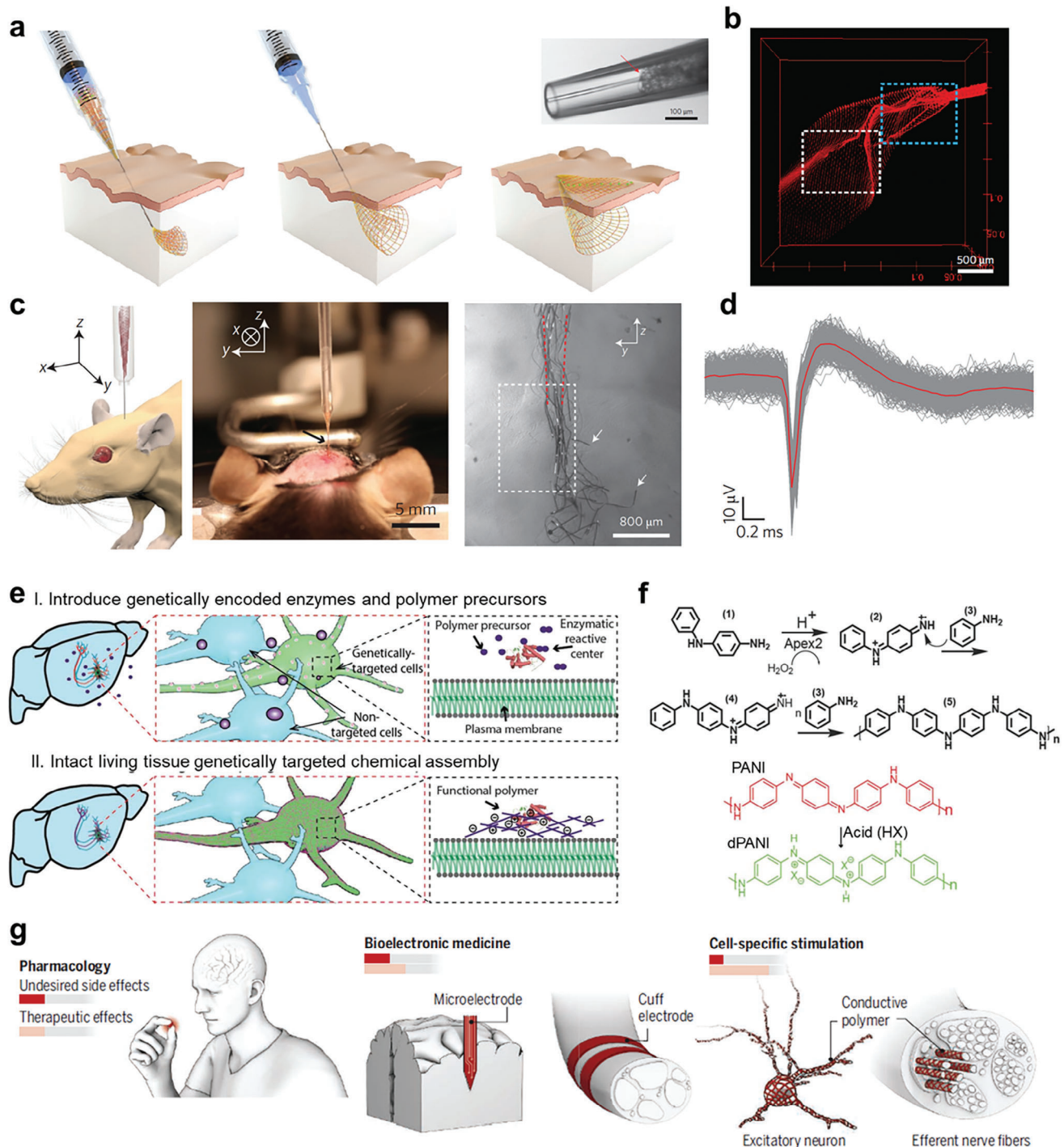


**Figure 9.** Injectable biocompatible materials. a) Schematic and microscope image of syringe-injectable mech electronics. b) 3D-reconstructed confocal fluorescence image of injected mesh electronics. c) Schematic and photograph of in vivo stereotaxic injection of mesh electrodes into a mouse brain (left) and microscope image of the mesh electronics in the hippocampus region five weeks post-injection (right). d) Superimposed single unit recordings from one channel after signal band-pass filtering (red: mean waveform). Reproduced with permission.<sup>[98]</sup> Copyright 2015, Springer Nature. e) Schematic of genetically targeted in vivo polymerization of functional materials. f) Chemical reactions of Apex2-mediated polymerization of conjugated polymer (polyaniline, PANI) and conversion of doped PANI (d-PANI) with acid treatment. Reproduced with permission.<sup>[100]</sup> Copyright 2020, American Association for the Advancement of Science. g) Schematics describing comparisons of neural modulation methods (pharmacology, bioelectronic medicine, and cell-specific stimulation) in terms of undesired side effects and therapeutic effects. Reproduced with permission.<sup>[101]</sup> Copyright 2020, American Association for the Advancement of Science.

and under various environmental conditions. Another important aspect is the integration of more complex functionalities into bio-integrated devices while ensuring biocompatibility.

## 5. Breathability

Breathability has emerged as a critical factor in wearable device technology, particularly in the context of continuous health monitoring, fitness tracking, and medical diagnostics. In such applications, wearer comfort is as paramount as device functionality. Furthermore, for prolonged usage, it is essential to account for the accumulation of skin by-products, such as sweat, which can disrupt the sensing capabilities and adhesion of bio-integrated devices to the skin, potentially causing skin-related issues such as irritation. Consequently, there has been a growing emphasis on breathability, leading to the proposal of various breathable systems based on porous structures for bio-integrated devices as a practical solution to address these challenges.

A skin-attachable device using a nanomesh (Figure 10a,b) is inflammation-free, gas-permeable, light weight, and stretchable.<sup>[24]</sup> The nanomesh platform is composed of gold-coated electrospun polyvinyl alcohol (PVA) nanofibers. The water-soluble ultrathin PVA nanomesh is easily dissolved by water vapor or sweat and then forms conformal skin contact with high ionic conductivity, thereby enabling highly accurate measurement of biosignals at the skin interface (Figure 10c). The nanomesh platform has distinctive geometrical advantages; It can significantly reduce the contact area between the device and skin. Moreover, its submicron pores allow the evaporation of sweat or vapor, thereby alleviating problems that can be induced by the blockage of these processes. The nanomesh platform was used as a strain-insensitive pressure sensor to monitor sophisticated finger manipulations with minimal mechanical constraints (Figure 10d,e).<sup>[23,25]</sup>

Recently, Yeon et al. reported a sweat pore-inspired perforated structure for better breathability of bio-integrated devices compared to a previous study based on vapor permeation systems (Figure 10f, top).<sup>[26]</sup> They presented an auxetic dumbbell-like perforated structure designed by a combination of hole pattern engineering and auxetic kirigami technology (Figure 10g,h), which enabled the complete permeation of sweat with synergistic effects on physical properties, including mechanical reliability under strain, skin conformability, areal mass density, and skin adhesion (Figure 10i,j). Finally, the perforated film was integrated with inorganic sensors (for temperature, hydration, strain, and ultra-violet light) to obtain fully breathable electronic skin devices (Figure 10f, bottom).

## 6. Biodegradability

Biodegradable electronic materials are centered on the development of electronic components and devices that can decompose naturally after their useful life, minimizing environmental impact and addressing the growing concern over electronic waste (e-waste).<sup>[102–105]</sup> This approach represents a significant shift toward sustainable electronics, integrating principles of green chemistry, environmental engineering, and materials science. Especially, transient inorganic and organic electronic materials that

can biodegrade over a period of usage are intensively being developed for bioresorbable implantable medical devices.<sup>[31,106–108]</sup>

### 6.1. Biodegradable Polymer Materials

The biodegradability of polymers can be tuned using molecular engineering.<sup>[109]</sup> Although many natural and synthetic biodegradable polymers have been reported, most of them exhibit insulating properties.<sup>[110–112]</sup> However, the development of biodegradable SPs is essential for fabricating biodegradable electronic devices.<sup>[108]</sup> Biocompatible and completely disintegrable SPs that utilize imine chemistry have been reported for use in ultrathin and ultralight weight transient electronics composed of disintegrable pseudo-CMOS circuits, while disintegrable SPs have been used in completely disintegrable transistors that can be fully degraded within 30 d in a buffer solution at pH 4.6.<sup>[113]</sup>

This concept was further developed for intrinsically stretchable and degradable semiconductor polymers. Intrinsic stretchability can improve the interface of a device with biological surfaces, such as tissues. One approach for fabricating intrinsically degradable and stretchable semiconductor films is to blend a degradable SP with an elastomer (Figure 11a).<sup>[114]</sup> SP with acid-labile imine bonds can be decomposed using acids and water. The polycaprolactone (PCL) groups in the elastomer backbone can disintegrate via hydrolysis and oxidation. A phase separation process causes the blended film of the semiconductor and elastomer to consist of nanoconfined semiconductor fibers in an elastomer matrix. This structure exhibited improved electrical properties and mechanical stretchability (Figure 11b).<sup>[114]</sup> This is a promising method to provide SPs with biodegradability and stretchability for use in implantable devices (Figure 11c).

Various electronic applications of biodegradable polymers have been reported. A biodegradable pressure sensor was applied to a flexible implant device.<sup>[115,116]</sup> A biodegradable and flexible arterial-pulse sensor system enables wireless monitoring of blood flow (Figure 11d).<sup>[117]</sup> This device has a capacitive pressure sensor that uses biodegradable polymers and an Mg inductive coil for wireless data transmission (Figure 11e). The pressure sensor had microstructured pyramids, which significantly increased pressure sensitivity. The arterial pulse was measured by converting the capacitance change from arterial pulsation to shift resonance, and the shift data were transferred wirelessly through the skin using an external reader coil. This biodegradable sensor worked successfully in an arterial occlusion test for monitoring blood pressure (Figure 11f).<sup>[117]</sup>

### 6.2. Biodegradable Inorganic Materials

Biodegradable inorganic materials, especially metals (magnesium, iron, and zinc) and semiconductors (silicone and germanium) have also gained significant interest in transient electronics for biomedical applications. These materials are designed to degrade safely within the body over time using hydrolysis chemistry, eliminating the need for a second surgery to remove implants and are also being explored for other environmentally sensitive applications.<sup>[118]</sup> The first physically transient inorganic electronic device was developed in 2012 to dissolve inorganic materials in aqueous solutions.<sup>[119]</sup> The device was a system-level

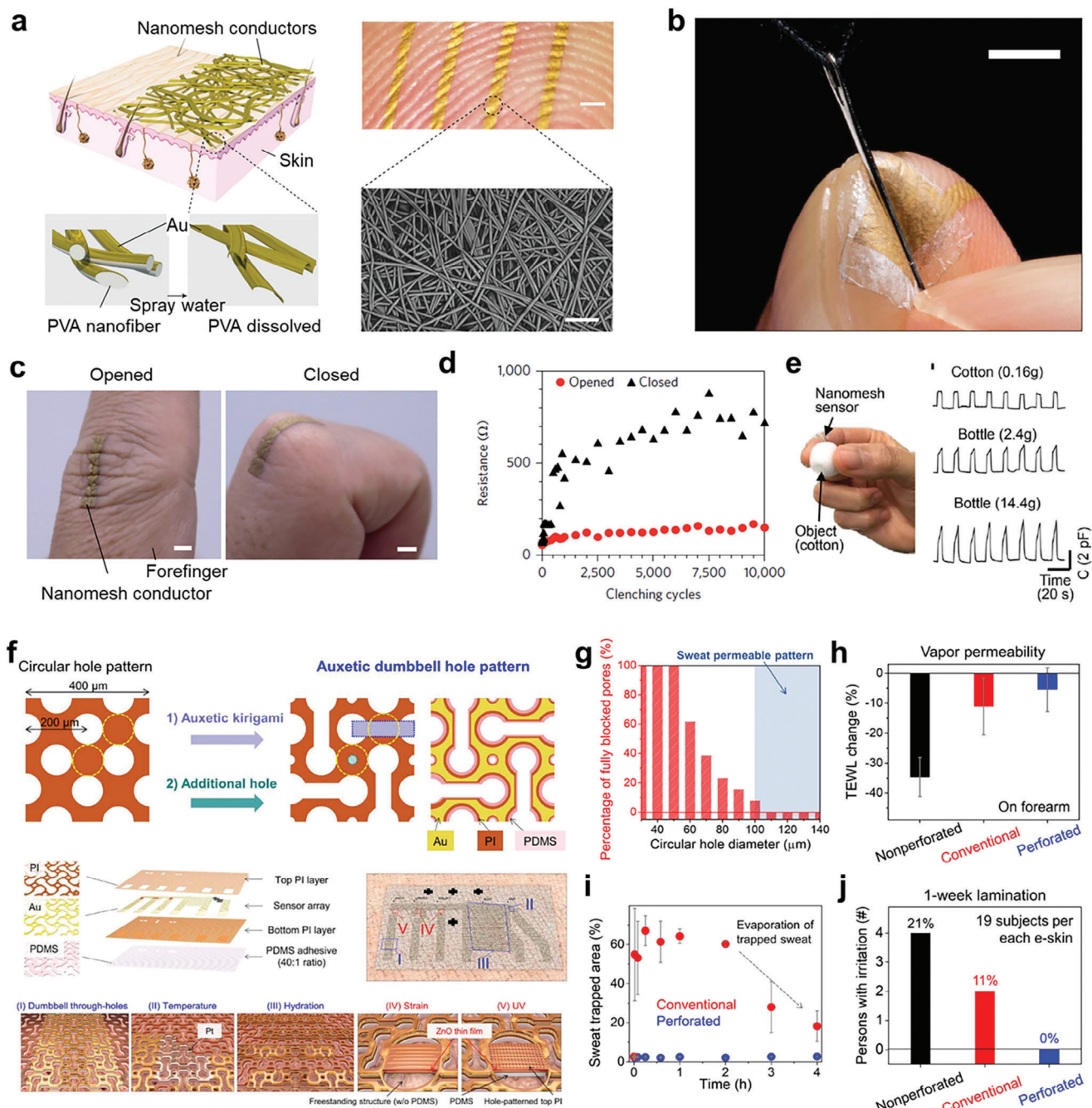


**Figure 10.** Breathable materials. a) Biocompatible nanomesh e-skin conductor attached to a finger print. b) Photograph of a nanomesh pressure sensor on the finger. Reproduced with permission.<sup>[24]</sup> Copyright 2017, Springer Nature. c) Photographs and d) resistance change of the nanomesh strain sensor on the finger when the finger is relaxed (opened) and bent (closed). e) Photograph and capacitance change of nanomesh pressure sensor on the fingers measuring the grip force for different soft objects (a cotton ball and small plastic bottles). Reproduced with permission.<sup>[23]</sup> Copyright 2020, American Association for the Advancement of Science. f) Schematic illustration of sweat pore-inspired perforated e-skin. g) Design of auxetic dumbbell through-holes with open channels on the sweat pore. h) Changes in transepidermal water loss (TEWL) of the forearm with e-skin. i) Areal changes of the sweat-trapped area after sweating. j) Skin compatibility of e-skins with 1-week lamination on the skin. Reproduced with permission.<sup>[26]</sup> Copyright 2021, American Association for the Advancement of Science.

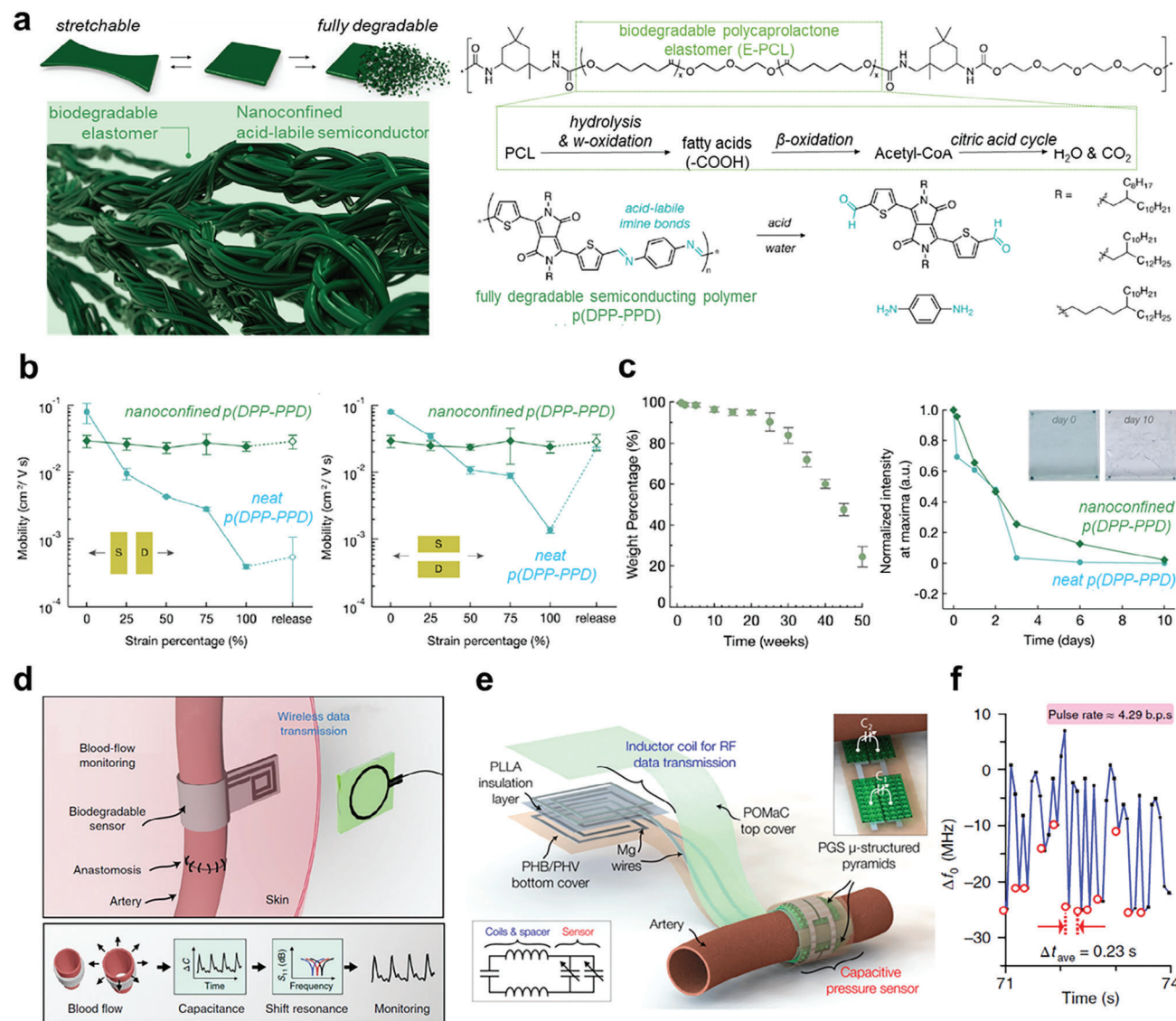


**Figure 11.** Biodegradable organic materials. a) Schematic of chemical structures and decomposition reactions of a stretchable and fully degradable polymer semiconductor embedded in biodegradable elastomer with nanoconfinement effect in an acidic environment. b) Change in carrier mobility of pure and nanoconfined p(DPP-PPD) under various strains in parallel (left) and perpendicular (right) directions. c) Degradation of E-PCL films with time (left) and gradual decrease of UV-Vis absorption spectra with time of the neat and nanoconfined polymer semiconductor films in 1 M trifluoroacetic acid (TFA, pH  $\approx$  0.5) in water (right). Reproduced with permission.<sup>[114]</sup> Copyright 2019, American Chemical Society. d) Schematic of the biodegradable and flexible arterial-pulse sensor system for wireless monitoring of blood flow. e) Schematic of system design with a cuff-type capacitive micropylamidal pulse sensor wrapping the artery, an inductor coil antenna for RF data transmission, and Mg wire interconnects. f) Measured change in frequency ( $\Delta f_0$ ) from the femoral artery (right). Reproduced with permission.<sup>[117]</sup> Copyright 2019, Springer Nature.

electronic circuit composed of a transistor, inductor, capacitor, diode, and resistor, all of which were fabricated using transient materials such as silicone as a semiconductor, Mg as a conductor, and MgO as a dielectric material on a water-soluble silk substrate (Figure 12a,b). All electronic components fabricated using silicone CMOS technologies worked as conventional devices and were completely dissolved within 10 min of hydrolysis in deionized water (Figure 12c). The transient bioresorbable device was evaluated for in vivo thermal therapy in mice.<sup>[119]</sup>

Subsequent studies further developed systems for transient electronics.<sup>[120–123]</sup> One is a wireless bioresorbable elec-

tronic system for nonpharmacological neuroregenerative therapy (Figure 12d).<sup>[124]</sup> The system includes a bioresorbable receiver antenna to obtain power wirelessly and is therefore appropriate for wireless programming of electrical stimulations for the management of nerve injuries.<sup>[124]</sup> The wireless bioresorbable electronic system was fabricated using Mg, Si, and SiO<sub>x</sub> on a biodegradable poly(lactic-co-glycolic acid) (PLGA) substrate. The device fully dissolves in  $\leq 25$  d in a phosphate-buffered saline (PBS) solution (pH = 7.4) at 37 °C (Figure 12e). A wireless and bioresorbable electronic system was successfully implanted and operated in a rodent for wireless electrical stimulation of the sci-



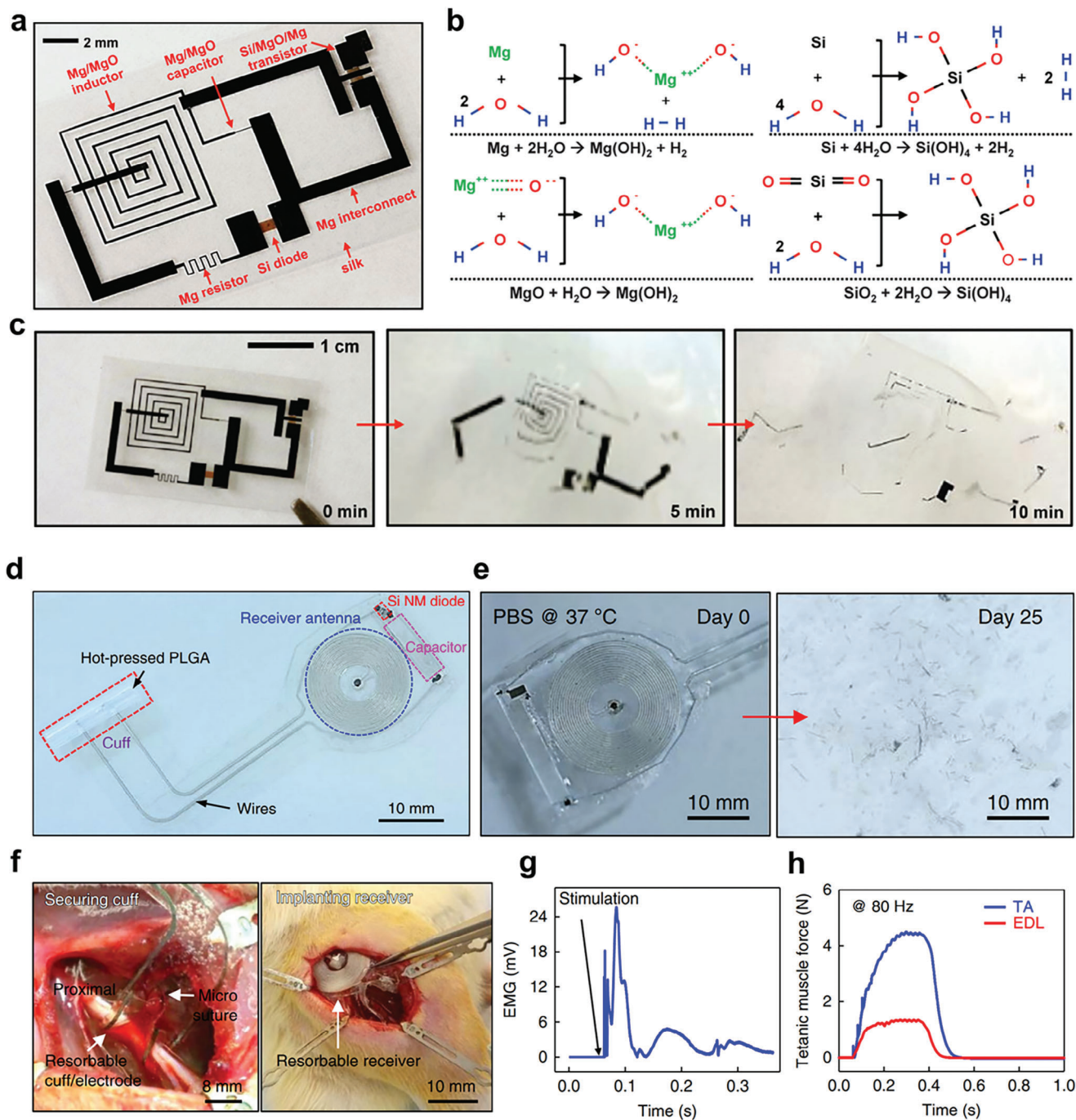


**Figure 12.** Biodegradable inorganic materials. a) Photograph of inorganic transient electronics. b) Chemical decomposition reaction of inorganic transient materials with water. c) Photographs of the decomposition of inorganic transient electronics in water. Reproduced with permission.<sup>[119]</sup> Copyright 2012, American Association for the Advancement of Science. d) Photograph of a bioresorbable wireless electrical stimulator. e) Photographs of degradation of a bioresorbable wireless stimulator in PBS (pH = 7.4) at 37 °C. f) Digital images of in vivo sciatic nerve stimulation. g) Electromyography signals and h) tetanic muscle force at the tibialis anterior muscles while stimulating the sciatic nerve. Reproduced with permission.<sup>[124]</sup> Copyright 2018, Springer Nature.

atic nerve, thereby accelerating the regeneration of injured nerves (Figure 12f–h).<sup>[124]</sup>

These biodegradable materials have demonstrated the potential of biodegradable electronic devices at the system level and offered promising alternatives to traditional permanent

metals in various applications, particularly in biomedical applications. Their ability to degrade in a controlled manner to non-toxic products that are safely metabolized or excreted by the body presents a significant advantage; However, the challenge still lies in optimizing their degradation rates, me-

chanical properties, and biological interactions for specific applications.

## 7. Conclusion and Outlook

As electronic devices have been developed toward improving users' convenience, especially in the aspect of portability from ENIAC to personal computers and even smartphones, electronic devices are expected to be integrated into the human body. To this end, functional electronic materials that can be seamlessly stacked on the skin but also even implanted in the human skin must be developed. We suggested five functionalities that skin-mountable electronic materials for bio-integrated e-skin devices should have: stretchability, self-healing ability, biocompatibility, breathability, and biodegradability, and described the current challenges for future research directions for each functionality.

Currently, lots of research is focusing on the development of new materials with these functionalities with an expectation of the potential applicability of the materials to next-generation bio-integrated electronic devices, but the devices are relatively non-specific yet. Therefore, along with the development of new materials with fundamental electrical properties (semiconducting, conducting, and insulating properties), the research of new practical bio-integrated applications is necessary to maximize the potential of the new functional materials. Based on five functionalities inspired by the human skin, the skin-mountable functional materials have the potential to revolutionize both existing and future applications. These materials could enhance current devices, like multimodal wearable sensors, health monitoring patches, and free-form displays. They also hold promise for unprecedented next-generation bio-integrated electronics, including skin-conformal augmented and virtual reality devices, soft neural interfaces, and energy-efficient neuromorphic bio-electronic devices.

## Acknowledgements

J.Y.O. and Y.L. contributed equally to this work. This work was supported by the National Research Foundation of Korea (NRF) grant funded by the Korea government (Ministry of Science and ICT) (NRF-2016R1A3B1908431, NRF-2022M3C1A3081211). This work was also supported by the National R&D Program through the National Research Foundation of Korea (NRF) funded by Ministry of Science and ICT (NRF-2021M3F3A2A01037858). Y.L. acknowledges Basic Science Research Program through the National Research Foundation of Korea (NRF) funded by the Ministry of Education (NRF-2021R1A6A3A03038934). J.Y.O. acknowledges National Research Foundation of Korea (NRF) grant funded by the Korean government (NRF-2021R1C1C1009925, NRF-2020R1A6A1A03048004, and 2019R1A6C101052), the GRR program of Gyeonggi province (GRRCKYUNGHEE2023-B03), and R&D program of the Ministry of Trade, Industry & Energy (No. 20012710 and No. 20015898) funded by the Korea Evaluation Institute of Industrial Technology (KEIT).

## Conflict of Interest

The authors declare no conflict of interest.

## Keywords

biocompatible materials, biodegradable materials, electronic skins, self-healable materials, stretchable materials

- [1] M. L. Hammock, A. Chortos, B. C. K. Tee, J. B. H. Tok, Z. Bao, *Adv. Mater.* **2013**, *25*, 5997.
- [2] S. Wang, J. Y. Oh, J. Xu, H. Tran, Z. Bao, *Acc. Chem. Res.* **2018**, *51*, 1033.
- [3] J. Y. Oh, Z. Bao, *Adv. Sci.* **2019**, *6*, 1900186.
- [4] J. C. Yang, J. Mun, S. Y. Kwon, S. Park, Z. Bao, S. Park, *Adv. Mater.* **2019**, *31*, 1904765.
- [5] A. Harris, M. Cooper, *Hum. Behav. Emerg. Technol.* **2019**, *1*, 15.
- [6] H. Jin, Y. S. Abu-Raya, H. Haick, *Adv. Healthcare Mater.* **2017**, *6*, 1700024.
- [7] S. M. Yun, M. Kim, Y. W. Kwon, H. Kim, M. J. Kim, Y.-G. Park, J.-U. Park, *Appl. Sci.* **2021**, *11*, 1235.
- [8] M. Straczekiewicz, P. James, J.-P. Onnela, *npj Digit. Med.* **2021**, *4*, 148.
- [9] S.-H. Sunwoo, K.-H. Ha, S. Lee, N. Lu, D.-H. Kim, *Annu. Rev. Chem. Biomol. Eng.* **2021**, *12*, 359.
- [10] H. Lim, H. S. Kim, R. Qazi, Y. Kwon, J. Jeong, W. Yeo, *Adv. Mater.* **2020**, *32*, 1901924.
- [11] D. C. Kim, H. J. Shim, W. Lee, J. H. Koo, D. Kim, *Adv. Mater.* **2020**, *32*, 1902743.
- [12] J. A. Rogers, T. Someya, Y. Huang, *Science* **2010**, *327*, 1603.
- [13] T. Someya, Z. Bao, G. G. Malliaras, *Nature* **2016**, *540*, 379.
- [14] B. Chu, W. Burnett, J. W. Chung, Z. Bao, *Nature* **2017**, *549*, 328.
- [15] Y. Liu, M. Pharr, G. A. Salvatore, *ACS Nano* **2017**, *11*, 9614.
- [16] S. Wang, J. Y. Oh, J. Xu, H. Tran, Z. Bao, *Acc. Chem. Res.* **2018**, *51*, 1033.
- [17] J. Y. Oh, Z. Bao, *Adv. Sci.* **2019**, *6*, 1900186.
- [18] S. Yao, Y. Zhu, *Adv. Mater.* **2015**, *27*, 1480.
- [19] T. Q. Trung, N.-E. Lee, *Adv. Mater.* **2017**, *29*, 1603167.
- [20] Y. Yang, M. W. Urban, *Chem. Soc. Rev.* **2013**, *42*, 7446.
- [21] S. Wang, M. W. Urban, *Nat. Rev. Mater.* **2020**, *5*, 562.
- [22] M. Irimia-Vladu, E. D. Głowacki, G. Voss, S. Bauer, N. S. Sariciftci, *Mater. Today* **2012**, *15*, 340.
- [23] S. Lee, S. Franklin, F. A. Hassani, T. Yokota, M. O. G. Nayeem, Y. Wang, R. Leib, G. Cheng, D. W. Franklin, T. Someya, *Science* **2020**, *370*, 966.
- [24] A. Miyamoto, S. Lee, N. F. Cooray, S. Lee, M. Mori, N. Matsuhisa, H. Jin, L. Yoda, T. Yokota, A. Itoh, M. Sekino, H. Kawasaki, T. Ebihara, M. Amagai, T. Someya, *Nat. Nanotechnol.* **2017**, *12*, 907.
- [25] Y. Wang, S. Lee, T. Yokota, H. Wang, Z. Jiang, J. Wang, M. Koizumi, T. Someya, *Sci. Adv.* **2020**, *eabb70*, eabb7043.
- [26] H. Yeon, H. Lee, Y. Kim, D. Lee, Y. Lee, J. S. Lee, J. Shin, C. Choi, J. H. Kang, J. M. Suh, H. Kim, H. S. Kum, J. Lee, D. Kim, K. Ko, B. S. Ma, P. Lin, S. Han, S. Kim, S. H. Bae, T. S. Kim, M. C. Park, Y. C. Joo, E. Kim, J. Han, J. Kim, *Sci. Adv.* **2021**, *7*, eabg8459.
- [27] Y. Kim, J. M. Suh, J. Shin, Y. Liu, H. Yeon, K. Qiao, H. S. Kum, C. Kim, H. E. Lee, C. Choi, H. Kim, D. Lee, J. Lee, J. H. Kang, B. I. Park, S. Kang, J. Kim, S. Kim, J. A. Perozek, K. Wang, Y. Park, K. Kishen, L. Kong, T. Palacios, J. Park, M. C. Park, H. J. Kim, Y. S. Lee, K. Lee, S. H. Bae, et al., *Science* **2022**, *377*, 859.
- [28] M. Irimia-Vladu, *Chem. Soc. Rev.* **2014**, *43*, 588.
- [29] Z. Terzopoulou, A. Zamboulis, I. Koumentakou, G. Michailidou, M. J. Noordam, D. N. Bikiaris, *Biomacromolecules* **2022**, *23*, 1841.
- [30] Y. Yang, T. Cui, D. Li, S. Ji, Z. Chen, W. Shao, H. Liu, T. L. Ren, *Nano-Micro Lett.* **2022**, *14*, 161.
- [31] V. R. Feig, H. Tran, Z. Bao, *ACS Cent. Sci.* **2018**, *4*, 337.
- [32] E. S. Hosseini, S. Dervin, P. Ganguly, R. Dahiya, *ACS Appl. Bio Mater.* **2021**, *4*, 163.
- [33] A. Chortos, J. Liu, Z. Bao, *Nat. Mater.* **2016**, *15*, 937.

- [34] Y. Dai, H. Hu, M. Wang, J. Xu, S. Wang, *Nat. Electron.* **2021**, *4*, 17.
- [35] H. Zhou, S. J. Han, A. K. Harit, D. H. Kim, D. Y. Kim, Y. S. Choi, H. Kwon, K. N. Kim, G. T. Go, H. J. Yun, B. H. Hong, M. C. Suh, S. Y. Ryu, H. Y. Woo, T. W. Lee, *Adv. Mater.* **2022**, *34*, 2203040.
- [36] H. Zhou, S. J. Han, H. D. Lee, D. Zhang, M. Anayee, S. H. Jo, Y. Gogotsi, T. W. Lee, *Adv. Mater.* **2022**, *34*, 2206377.
- [37] Y. Lee, J. W. Chung, G. H. Lee, H. Kang, J.-Y. Kim, C. Bae, H. Yoo, S. Jeong, H. Cho, S.-G. Kang, J. Y. Jung, D.-W. Lee, S. Gam, S. G. Hahm, Y. Kuzumoto, S. J. Kim, Z. Bao, Y. Hong, Y. Yun, S. Kim, *Sci. Adv.* **2021**, *7*, eabg9180.
- [38] D.-H. Kim, N. Lu, R. Ma, Y.-S. Kim, R.-H. Kim, S. Wang, J. Wu, S. M. Won, H. Tao, A. Islam, K. J. Yu, T. Kim, R. Chowdhury, M. Ying, L. Xu, M. Li, H.-J. Chung, H. Keum, M. McCormick, P. Liu, Y.-W. Zhang, F. G. Omenetto, Y. Huang, T. Coleman, J. A. Rogers, *Science* **2011**, *333*, 838.
- [39] S. Choi, H. Lee, R. Ghaffari, T. Hyeon, D.-H. Kim, *Adv. Mater.* **2016**, *28*, 4203.
- [40] S. J. Han, H. Zhou, H. Kwon, S. J. Woo, T. W. Lee, *Adv. Funct. Mater.* **2023**, *33*, 2211150.
- [41] N. Matsuhisa, X. Chen, Z. Bao, T. Someya, *Chem. Soc. Rev.* **2019**, *48*, 2946.
- [42] Y. Lee, H. Zhou, T.-W. Lee, *J. Mater. Chem. C* **2018**, *6*, 3538.
- [43] Y. Lee, H. Cho, H. Yoon, H. Kang, H. Yoo, H. Zhou, S. Jeong, G. H. Lee, G. Kim, G. T. Go, J. Seo, T. W. Lee, Y. Hong, Y. Yun, *Adv. Mater. Technol.* **2023**, *8*, 2201067.
- [44] J. Kim, M. Lee, H. J. Shim, R. Ghaffari, H. R. Cho, D. Son, Y. H. Jung, M. Soh, C. Choi, S. Jung, K. Chu, D. Jeon, S.-T. Lee, J. H. Kim, S. H. Choi, T. Hyeon, D.-H. Kim, *Nat. Commun.* **2014**, *5*, 5747.
- [45] M. Kaltenbrunner, T. Sekitani, J. Reeder, T. Yokota, K. Kuribara, T. Tokuhara, M. Drack, R. Schwödiauer, I. Graz, S. Bauer-Gogonea, S. Bauer, T. Someya, *Nature* **2013**, *499*, 458.
- [46] D.-H. Kim, J. Xiao, J. Song, Y. Huang, J. A. Rogers, *Adv. Mater.* **2010**, *22*, 2108.
- [47] B. Wang, S. Bao, S. Vinnikova, P. Ghanta, S. Wang, *npj Flex. Electron.* **2017**, *1*, 5.
- [48] Y. Lee, J. Y. Oh, T. R. Kim, X. Gu, Y. Kim, G. N. Wang, H. Wu, R. Pfaltner, J. W. F. To, T. Katsumata, D. Son, J. Kang, J. R. Matthews, W. Niu, M. He, R. Sinclair, Y. Cui, J. B.-H. Tok, T. Lee, Z. Bao, *Adv. Mater.* **2018**, *30*, 1704401.
- [49] Y. Lee, J. Y. Oh, W. Xu, O. Kim, T. R. Kim, J. Kang, Y. Kim, D. Son, J. B. H. Tok, M. J. Park, Z. Bao, T.-W. Lee, *Sci. Adv.* **2018**, *4*, eaat7387.
- [50] Y. Lee, Y. Liu, D.-G. Seo, J. Y. Oh, Y. Kim, J. Li, J. Kang, J. Kim, J. Mun, A. M. Foudeh, Z. Bao, T.-W. Lee, *Nat. Biomed. Eng.* **2022**, *7*, 511.
- [51] J. Xu, S. Wang, G.-J. N. Wang, C. Zhu, S. Luo, L. Jin, X. Gu, S. Chen, V. R. Feig, J. W. F. To, S. Rondeau-Gagné, J. Park, B. C. Schroeder, C. Lu, J. Y. Oh, Y. Wang, Y. Kim, H. Yan, R. Sinclair, D. Zhou, G. Xue, B. Murmann, C. Linder, W. Cai, J. B.-H. Tok, J. W. Chung, Z. Bao, *Science* **2017**, *355*, 59.
- [52] S. Wang, J. Xu, W. Wang, G.-J. N. Wang, R. Rastak, F. Molina-Lopez, J. W. Chung, S. Niu, V. R. Feig, J. Lopez, T. Lei, S.-K. Kwon, Y. Kim, A. M. Foudeh, A. Ehrlich, A. Gasperini, Y. Yun, B. Murmann, J. B. H. Tok, Z. Bao, *Nature* **2018**, *555*, 83.
- [53] J. Xu, H.-C. Wu, C. Zhu, A. Ehrlich, L. Shaw, M. Nikolka, S. Wang, F. Molina-Lopez, X. Gu, S. Luo, D. Zhou, Y.-H. Kim, G.-J. N. Wang, K. Gu, V. R. Feig, S. Chen, Y. Kim, T. Katsumata, Y.-Q. Zheng, H. Yan, J. W. Chung, J. Lopez, B. Murmann, Z. Bao, *Nat. Mater.* **2019**, *18*, 594.
- [54] G.-J. N. Wang, L. Shaw, J. Xu, T. Kurosawa, B. C. Schroeder, J. Y. Oh, S. J. Benight, Z. Bao, *Adv. Funct. Mater.* **2016**, *26*, 7254.
- [55] J. Y. Oh, S. Rondeau-Gagné, Y.-C. Chiu, A. Chortos, F. Lissel, G.-J. N. Wang, B. C. Schroeder, T. Kurosawa, J. Lopez, T. Katsumata, J. Xu, C. Zhu, X. Gu, W.-G. Bae, Y. Kim, L. Jin, J. W. Chung, J. B. H. Tok, Z. Bao, *Nature* **2016**, *539*, 411.
- [56] S. Lanone, P. Andujar, A. Kermanizadeh, J. Boczkowski, *Adv. Drug Deliv. Rev.* **2013**, *65*, 2063.
- [57] C. P. Firme, P. R. Bandaru, *Nanomed. Nanotechnol. Biol. Med.* **2010**, *6*, 245.
- [58] Y. Liu, Y. Zhao, B. Sun, C. Chen, *Acc. Chem. Res.* **2013**, *46*, 702.
- [59] M. H. Kim, M. W. Jeong, J. S. Kim, T. U. Nam, N. T. P. Vo, L. Jin, T. Il Lee, J. Y. Oh, *Sci. Adv.* **2022**, *8*, eade2988.
- [60] J. Y. Oh, D. Son, T. Katsumata, Y. Lee, Y. Kim, J. Lopez, H.-C. Wu, J. Kang, J. Park, X. Gu, J. Mun, N. G.-J. Wang, Y. Yin, W. Cai, Y. Yun, J. B. H. Tok, Z. Bao, *Sci. Adv.* **2019**, *5*, eaav3097.
- [61] J. H. Koo, J. Kang, S. Lee, J.-K. Song, J. Choi, J. Yoon, H. J. Park, S.-H. Sunwoo, D. C. Kim, W. Nam, D.-H. Kim, S. G. Im, D. Son, *Nat. Electron.* **2023**, *6*, 137.
- [62] Y.-Q. Zheng, Y. Liu, D. Zhong, S. Nikzad, S. Liu, Z. Yu, D. Liu, H.-C. Wu, C. Zhu, J. Li, H. Tran, J. B. H. Tok, Z. Bao, *Science* **2021**, *373*, 88.
- [63] J. F. Chang, M. C. Gwinner, M. Caironi, T. Sakanoue, H. Siringhaus, *Adv. Funct. Mater.* **2010**, *20*, 2825.
- [64] P. E. Malinowski, A. Nakamura, D. Janssen, Y. Kamochi, I. Koyama, Y. Iwai, A. Stefaniuk, E. Wilenska, C. Salas Redondo, D. Cheyns, S. Steudel, P. Heremans, *Org. Electron.* **2014**, *15*, 2355.
- [65] Y. Jiang, Z. Zhang, Y.-X. Wang, D. Li, C.-T. Coen, E. Hwaun, G. Chen, H.-C. Wu, D. Zhong, S. Niu, W. Wang, A. Saberi, J.-C. Lai, Y. Wu, Y. Wang, A. A. Trotsyuk, K. Y. Loh, C.-C. Shih, W. Xu, K. Liang, K. Zhang, Y. Bai, G. Gurusankar, W. Hu, W. Jia, Z. Cheng, R. H. Dauskardt, G. C. Gurtner, J. B. H. Tok, K. Deisseroth, et al., *Science* **2022**, *375*, 1411.
- [66] J. C. Cremaldi, B. Bhushan, *Beilstein J. Nanotechnol.* **2018**, *9*, 907.
- [67] J. Kang, J. B. H. Tok, Z. Bao, *Nat. Electron.* **2019**, *2*, 144.
- [68] S. H. Cho, S. R. White, P. V. Braun, *Adv. Mater.* **2009**, *21*, 645.
- [69] K. S. Toohey, N. R. Sottos, J. A. Lewis, J. S. Moore, S. R. White, *Nat. Mater.* **2007**, *6*, 581.
- [70] C. J. Hansen, W. Wu, K. S. Toohey, N. R. Sottos, S. R. White, J. A. Lewis, *Adv. Mater.* **2009**, *21*, 4143.
- [71] C. E. Diesendruck, N. R. Sottos, J. S. Moore, S. R. White, *Angew. Chem.* **2015**, *127*, 10572.
- [72] E. J. Markvicka, M. D. Bartlett, X. Huang, C. Majidi, *Nat. Mater.* **2018**, *17*, 618.
- [73] Y. Li, T. Fang, J. Zhang, H. Zhu, Y. Sun, S. Wang, Y. Lu, D. Kong, *Proc Natl Acad Sci U S A* **2023**, *120*, 2017.
- [74] Z. Wei, J. H. Yang, J. Zhou, F. Xu, M. Zrinyi, P. H. Dussault, Y. Osada, Y. M. Chen, *Chem. Soc. Rev.* **2014**, *43*, 8114.
- [75] N. Roy, B. Bruchmann, J.-M. Lehn, *Chem. Soc. Rev.* **2015**, *44*, 3786.
- [76] T. Huynh, P. Sonar, H. Haick, *Adv. Mater.* **2017**, *29*, 1604973.
- [77] J. Kang, D. Son, G. N. Wang, Y. Liu, J. Lopez, Y. Kim, J. Y. Oh, T. Katsumata, J. Mun, Y. Lee, L. Jin, J. B.-H. Tok, Z. Bao, *Adv. Mater.* **2018**, *30*, 1706846.
- [78] T. Matsuda, R. Kawakami, R. Namba, T. Nakajima, J. P. Gong, *Science* **2019**, *363*, 504.
- [79] W. Bin Ying, G. Wang, Z. Kong, C. K. Yao, Y. Wang, H. Hu, F. Li, C. Chen, Y. Tian, J. Zhang, R. Zhang, J. Zhu, *Adv. Funct. Mater.* **2021**, *31*, 2009869.
- [80] C. B. Cooper, S. E. Root, L. Michalek, S. Wu, J. C. Lai, M. Khatib, S. T. Oyakhire, R. Zhao, J. Qin, Z. Bao, *Science* **2023**, *380*, 935.
- [81] D. T. Simon, E. O. Gabrielsson, K. Tybrandt, M. Berggren, *Chem. Rev.* **2016**, *116*, 13009.
- [82] E. Song, J. Li, S. M. Won, W. Bai, J. A. Rogers, *Nat. Mater.* **2020**, *19*, 590.
- [83] G. T. Go, Y. Lee, D. G. Seo, T. W. Lee, *Adv. Mater.* **2022**, *34*, 2201864.
- [84] H. Wu, G. Yang, K. Zhu, S. Liu, W. Guo, Z. Jiang, Z. Li, *Adv. Sci.* **2021**, *8*, 2001938.
- [85] S. G. Higgins, A. Lo Fiego, I. Patrick, A. Creamer, M. M. Stevens, *Adv. Mater. Technol.* **2020**, *5*, 2000384.
- [86] D.-L. Wen, D.-H. Sun, P. Huang, W. Huang, M. Su, Y. Wang, M.-D. Han, B. Kim, J. Brugger, H.-X. Zhang, X.-S. Zhang, *Microsyst. Nanoeng.* **2021**, *7*, 35.
- [87] H. Yuk, B. Lu, X. Zhao, *Chem. Soc. Rev.* **2019**, *48*, 1642.

- [88] Q. Peng, J. Chen, T. Wang, X. Peng, J. Liu, X. Wang, J. Wang, H. Zeng, *InfoMat* **2020**, 2, 843.
- [89] S. Oribe, S. Yoshida, S. Kusama, S. Osawa, A. Nakagawa, M. Iwasaki, T. Tominaga, M. Nishizawa, *Sci. Rep.* **2019**, 9, 13379.
- [90] Y. Liu, V. R. Feig, Z. Bao, *Adv. Healthcare Mater.* **2021**, 10, 2001916.
- [91] J. Liu, X. Zhang, Y. Liu, M. Rodrigo, P. D. Loftus, J. Aparicio-Valenzuela, J. Zheng, T. Pong, K. J. Cyr, M. Babakhanian, J. Hasi, J. Li, Y. Jiang, C. J. Kenney, P. J. Wang, A. M. Lee, Z. Bao, *Proc. Natl. Acad. Sci. U. S. A.* **2020**, 117, 14769.
- [92] P. Jastrzebska-Perfect, S. Chowdhury, G. D. Spyropoulos, Z. Zhao, C. Cea, J. N. Gelinis, D. Khodagholy, *Adv. Funct. Mater.* **2020**, 30, 1909165.
- [93] S. M. Won, E. Song, J. Zhao, J. Li, J. Rivnay, J. A. Rogers, *Adv. Mater.* **2018**, 30, 1800534.
- [94] J. Rivnay, H. Wang, L. Fenno, K. Deisseroth, G. G. Malliaras, *Sci. Adv.* **2017**, 3, e1601649.
- [95] X. Gu, S. Y. Yeung, A. Chadda, E. N. Y. Poon, K. R. Boheler, I.-M. Hsing, *Adv. Biosyst.* **2019**, 3, 1800248.
- [96] Y. Liu, J. Liu, S. Chen, T. Lei, Y. Kim, S. Niu, H. Wang, X. Wang, A. M. Foudeh, J. B. H. Tok, Z. Bao, *Nat. Biomed. Eng.* **2019**, 3, 58.
- [97] Y. Liu, J. Li, S. Song, J. Kang, Y. Tsao, S. Chen, V. Mottini, K. McConnell, W. Xu, Y.-Q. Zheng, J. B. H. Tok, P. M. George, Z. Bao, *Nat. Biotechnol.* **2020**, 38, 1031.
- [98] J. Liu, T.-M. Fu, Z. Cheng, G. Hong, T. Zhou, L. Jin, M. Duvvuri, Z. Jiang, P. Kruskal, C. Xie, Z. Suo, Y. Fang, C. M. Lieber, *Nat. Nanotechnol.* **2015**, 10, 629.
- [99] T. Zhou, G. Hong, T.-M. Fu, X. Yang, T. G. Schuhmann, R. D. Viveros, C. M. Lieber, *Proc. Natl. Acad. Sci. U. S. A.* **2017**, 114, 5894.
- [100] J. Liu, Y. S. Kim, C. E. Richardson, A. Tom, C. Ramakrishnan, F. Birey, T. Katsumata, S. Chen, C. Wang, X. Wang, L.-M. Joubert, Y. Jiang, H. Wang, L. E. Fenno, J. B. H. Tok, S. P. Pasca, K. Shen, Z. Bao, K. Deisseroth, *Science* **2020**, 367, 1372.
- [101] K. J. Otto, C. E. Schmidt, *Science* **2020**, 367, 1303.
- [102] P. Kiddee, R. Naidu, M. H. Wong, *Waste Manag.* **2013**, 33, 1237.
- [103] Z. Wang, B. Zhang, D. Guan, *Nature* **2016**, 536, 23.
- [104] M. Kaya, *Waste Manag.* **2016**, 57, 64.
- [105] P. Tanskanen, *Acta Mater.* **2013**, 61, 1001.
- [106] R. Li, L. Wang, D. Kong, L. Yin, *Bioact. Mater.* **2018**, 3, 322.
- [107] W. Li, Q. Liu, Y. Zhang, C. Li, Z. He, W. C. H. Choy, P. J. Low, P. Sonar, A. K. K. Kyaw, *Adv. Mater.* **2020**, 32, 2001591.
- [108] S.-W. Hwang, G. Park, H. Cheng, J.-K. Song, S.-K. Kang, L. Yin, J.-H. Kim, F. G. Omenetto, Y. Huang, K.-M. Lee, J. A. Rogers, *Adv. Mater.* **2014**, 26, 1992.
- [109] H. Tran, V. R. Feig, K. Liu, Y. Zheng, Z. Bao, *Macromolecules* **2019**, 52, 3965.
- [110] I. Armentano, M. Dottori, E. Fortunati, S. Mattioli, J. M. Kenny, *Polym. Degrad. Stab.* **2010**, 95, 2126.
- [111] V. Siracusa, P. Rocculi, S. Romani, M. D. Rosa, *Trends Food Sci. Technol.* **2008**, 19, 634.
- [112] Y. Li, D. Maciel, J. Rodrigues, X. Shi, H. Tomás, *Chem. Rev.* **2015**, 115, 8564.
- [113] T. Lei, M. Guan, J. Liu, H.-C. Lin, R. Pfattner, L. Shaw, A. F. McGuire, T.-C. Huang, L. Shao, K.-T. Cheng, J. B. H. Tok, Z. Bao, *Proc. Natl. Acad. Sci. U. S. A.* **2017**, 114, 5107.
- [114] H. Tran, V. R. Feig, K. Liu, H.-C. Wu, R. Chen, J. Xu, K. Deisseroth, Z. Bao, *ACS Cent. Sci.* **2019**, 5, 1884.
- [115] C. M. Boutry, A. Nguyen, Q. O. Lawal, A. Chortos, S. Rondeau-Gagné, Z. Bao, *Adv. Mater.* **2015**, 27, 6954.
- [116] C. M. Boutry, Y. Kaizawa, B. C. Schroeder, A. Chortos, A. Legrand, Z. Wang, J. Chang, P. Fox, Z. Bao, *Nat. Electron.* **2018**, 1, 314.
- [117] C. M. Boutry, L. Beker, Y. Kaizawa, C. Vassos, H. Tran, A. C. Hinckley, R. Pfattner, S. Niu, J. Li, J. Claverie, Z. Wang, J. Chang, P. M. Fox, Z. Bao, *Nat. Biomed. Eng.* **2019**, 3, 47.
- [118] R. Singh, M. J. Bathaei, E. Istif, L. Beker, *Adv. Healthcare Mater.* **2020**, 9, 2000790.
- [119] S.-W. Hwang, H. Tao, D.-H. Kim, H. Cheng, J.-K. Song, E. Rill, M. A. Brenckle, B. Panilaitis, S. M. Won, Y.-S. Kim, Y. M. Song, K. J. Yu, A. Ameen, R. Li, Y. Su, M. Yang, D. L. Kaplan, M. R. Zakin, M. J. Slepian, Y. Huang, F. G. Omenetto, J. A. Rogers, *Science* **2012**, 337, 1640.
- [120] Y. S. Choi, R. T. Yin, A. Pfenniger, J. Koo, R. Avila, K. Benjamin Lee, S. W. Chen, G. Lee, G. Li, Y. Qiao, A. Murillo-Berlioz, A. Kiss, S. Han, S. M. Lee, C. Li, Z. Xie, Y.-Y. Chen, A. Burrell, B. Geist, H. Jeong, J. Kim, H.-J. Yoon, A. Banks, S.-K. Kang, Z. J. Zhang, C. R. Haney, A. V. Sahakian, D. Johnson, T. Efimova, Y. Huang, et al., *Nat. Biotechnol.* **2021**, 39, 1228.
- [121] S.-W. Hwang, C. H. Lee, H. Cheng, J.-W. Jeong, S.-K. Kang, J.-H. Kim, J. Shin, J. Yang, Z. Liu, G. A. Ameer, Y. Huang, J. A. Rogers, *Nano Lett.* **2015**, 15, 2801.
- [122] J.-S. Shim, J. A. Rogers, S.-K. Kang, *Mater. Sci. Eng. R Rep.* **2021**, 145, 100624.
- [123] K. K. Fu, Z. Wang, J. Dai, M. Carter, L. Hu, *Chem. Mater.* **2016**, 28, 3527.
- [124] J. Koo, M. R. MacEwan, S.-K. Kang, S. M. Won, M. Stephen, P. Gamble, Z. Xie, Y. Yan, Y.-Y. Chen, J. Shin, N. Birenbaum, S. Chung, S. B. Kim, J. Khalifeh, D. V. Harburg, K. Bean, M. Paskett, J. Kim, Z. S. Zohny, S. M. Lee, R. Zhang, K. Luo, B. Ji, A. Banks, H. M. Lee, Y. Huang, W. Z. Ray, J. A. Rogers, *Nat. Med.* **2018**, 24, 1830.



**Jin Young Oh** is an assistant professor in the Department of Chemical Engineering at Kyung Hee University, South Korea. He received his M.S. in the Department of Chemistry from Yonsei University in 2008 and earned his Ph.D. in Materials Science and Engineering from Yonsei University, South Korea, in 2014. He joined Stanford University, USA, as a postdoctoral fellow from 2015 to 2018. His current research focuses on developing intrinsically stretchable and self-healable semiconductor devices (circuit, memory, display, sensor, and power supply) for skin electronics.



**Yeongjun Lee** is an assistant professor in the Department of Brain and Cognitive Science at KAIST. He received his Ph.D. in the Department of Materials Science and Engineering (MSE) from Pohang University of Science and Technology (POSTECH), South Korea in 2018. He worked in MSE at Seoul National University as a postdoctoral researcher and Material Research Center in Samsung Advanced Institute of Technology as a staff researcher (2019–2021). After that, he joined Stanford University, USA, as a postdoctoral researcher (2021–2024). His research interests include soft materials and devices for brain-machine interfaces, stretchable/wearable electronics, and low-power neuromorphic applications.



**Tae-Woo Lee** is a professor in the Department of MSE at Seoul National University, South Korea. He received his Ph.D. in Chemical Engineering from KAIST, South Korea in 2002. He joined Bell Laboratories, USA, as a postdoctoral researcher and worked at Samsung Advanced Institute of Technology as a member of the research staff (2003–2008). He was an associate professor in MSE at Pohang University of Science and Technology (POSTECH), South Korea, until August 2016. His research focuses on printed or soft electronics that use organic and organic-inorganic hybrid materials for flexible/stretchable displays, solid-state lighting, solar energy conversion devices, and bioinspired neuromorphic devices.